

Accelerator Mass Spectrometry Measurements of Plutonium in Sediment and Seawater from the Marshall Islands

M. Leisvik
Thesis for Master of Science Degree

August 1, 2001

U.S. Department of Energy

Lawrence
Livermore
National
Laboratory

DISCLAIMER

This document was prepared as an account of work sponsored by an agency of the United States Government. Neither the United States Government nor the University of California nor any of their employees, makes any warranty, express or implied, or assumes any legal liability or responsibility for the accuracy, completeness, or usefulness of any information, apparatus, product, or process disclosed, or represents that its use would not infringe privately owned rights. Reference herein to any specific commercial product, process, or service by trade name, trademark, manufacturer, or otherwise, does not necessarily constitute or imply its endorsement, recommendation, or favoring by the United States Government or the University of California. The views and opinions of authors expressed herein do not necessarily state or reflect those of the United States Government or the University of California, and shall not be used for advertising or product endorsement purposes.

This work was performed under the auspices of the U. S. Department of Energy by the University of California, Lawrence Livermore National Laboratory under Contract No. W-7405-Eng-48.

This report has been reproduced
directly from the best available copy.

Available to DOE and DOE contractors from the
Office of Scientific and Technical Information
P.O. Box 62, Oak Ridge, TN 37831
Prices available from (423) 576-8401
<http://apollo.osti.gov/bridge/>

Available to the public from the
National Technical Information Service
U.S. Department of Commerce
5285 Port Royal Rd.,
Springfield, VA 22161
<http://www.ntis.gov/>

OR

Lawrence Livermore National Laboratory
Technical Information Department's Digital Library
<http://www.llnl.gov/tid/Library.html>

Accelerator Mass Spectrometry Measurements of Plutonium in Sediment and Seawater from the Marshall Islands

- A final paper for a Master of Science Degree in Radioecology at Lund University -

Mathias Leisvik

Lund University,
Department of Radiation physics,
Lund

Supervisor: Dr. Elis Holm, Radiation Physics department, Lund University, Lund,
Sweden

Opponents: Dr. Terry Hamilton, Marshall Islands Dose Assessment and Radioecology
Program, LLNL, Livermore, U.S.A.

Doc. Ragnar Hellborg, Department of Physics, Lund University, Lund,
Sweden

INTRODUCTION	3
THEORETICAL AND TECHNICAL BACKGROUND	4
Plutonium	4
Nuclear bombs	7
Fission bombs	7
Thermonuclear explosives	7
Post detonation of nuclear bombs	8
Nuclear bomb testing in the Marshall Islands	9
The history of the Marshall Islands as a nuclear weapons test area	9
The Castle Bravo incident	9
Accelerator Mass Spectrometry (AMS) for Plutonium Measurements	11
History	11
Applications for AMS	12
Important steps in AMS	12
Ion source	13
Low energy mass analysis	13
Tandem electrostatic accelerator	15
High energy analysis	15
Detector	16
Other	16
Preparations and performances for plutonium measurements with AMS	17
Sample preparation	17
Tuning	17
Efficiency	17
Detection limits	18
Background levels	18
Precision	19
 PART 1: MEASUREMENT OF PLUTONIUM IN SEDIMENT FROM THE RONGELAP ATOLL USING AMS.	 20
Background	20
Method	24
Sampling	24
Chemical preparation	26
Analysis	28
Results	29
Blanks and IAEA-367 standard sediment samples	29
Surface sediment	30
Sediment cores	35
Discussion	39

PART 2: MEASUREMENT OF PLUTONIUM IN SEAWATER FROM THE MARSHALL ISLANDS USING AMS	41
Background	41
Method	41
Sampling	41
Chemical preparation	43
General	43
Fluride precipitation	43
Tests	43
Analysis	45
Results	46
Discussion	48
 ACKNOWLEDGEMENT	 49
 REFERENCES	 50
 APPENDIX I: FLUORIDE PRECIPITATION ON SEA WATER SAMPLES	 53
 APPENDIX II: RESULTS FOR THE SEDIMENT SAMPLES	 55
 APPENDIX III: THE RONGELAP AND THE BIKINI ATOLL	 57

Introduction

During the summer 2000, I was given the opportunity to work for about three months as a technical trainee at Lawrence Livermore National Laboratory, or LLNL as I will refer to it hereafter. University of California runs this Department of Energy laboratory, which is located 70 km east of San Francisco, in the small city of Livermore. This master thesis in Radioecology is based on the work I did here.

LLNL, as a second U.S.-facility for development of nuclear weapons, was built in Livermore in the beginning of the 1950:s (Los Alamos in New Mexico was the other one). It has since then also become a “science centre” for a number of areas like magnetic and laser fusion energy, non-nuclear energy, biomedicine, and environmental science. The Laboratory's mission has changed over the years to meet new national needs. The following two statements were found on the homepage of LLNL (<http://www.llnl.gov>), at 2001-03-05, where also information about the laboratory and the scientific projects that takes place there, can be found.

“Our primary mission is to ensure that the nation's nuclear weapons remain safe, secure, and reliable and to prevent the spread and use of nuclear weapons worldwide”.

“Our goal is to apply the best science and technology to enhance the security and well-being of the nation and to make the world a safer place.”

The Marshall Islands Dose Assessment and Radioecology group at the Health and Ecological Assessments division employed me, and I also worked to some extent with the Centre for Accelerator Mass Spectrometry (CAMS) group. The work I did at LLNL can be divided into two parts. In the first part Plutonium (Pu) measurements in sediments from the Rongelap atoll in Marshall Islands, using Accelerator Mass Spectrometry (AMS) were done. The method for measuring these kinds of samples is well understood at LLNL since soil samples have been measured with AMS for Pu in the past. Therefore it was the results that were of main interest and not the technique. The second part was to take advantage of AMS's very high sensitivity by measure the Pu-concentrations in small volumes (0.04 – 1 L) of seawater. The technique for using AMS at Pu-measurements in seawater is relatively new and the main task for me was to find out a method that could work in practice. The area where the sediment samples and the water samples were collected are high above background levels for many radionuclides, including Pu, because of the detonation of the nuclear bomb code-named Castle Bravo, in 1954.

Theoretical and Technical Background

Plutonium

Plutonium was discovered in 1940 by the American chemists Glenn T. Seaborg and Edwin M. McMillan. Since its discovery it has become one of the most thoroughly studied of all elements and yet one of those we know least about (Pentreath 1995). The element has atomic number 92 and 15 isotopes with mass numbers ranging from 232 to 246. The properties of the environmentally most important plutonium isotopes, ^{238}Pu , ^{239}Pu , ^{240}Pu and ^{241}Pu , as well as of ^{241}Am , are found in table 1. All of these isotopes except ^{241}Pu decay by alpha emission. ^{241}Pu decay by beta to ^{241}Am , which in turn decay by alpha emission (Pentreath 1995).

Isotope	Main decay mode	Half-life	Q_α - energy
^{238}Pu	α	87.73 a	5.59 MeV
^{239}Pu	α	24,110 a	5.24 MeV
^{240}Pu	α	6,563 a	5.26 MeV
^{241}Pu	β	14.4 a	-
^{241}Am	α	432.2 a	5.64 MeV

Table 1: Properties of some of the environmentally most important plutonium isotopes and ^{241}Am (Firestone, 1996)

Both ^{239}Pu and ^{241}Pu are fissile (they can be split by both slow and fast neutrons with the accompanying release of energy and more neutrons), but of practical reasons, only ^{239}Pu can be used as fuel and in weapons. All the plutonium isotopes are unstable and exist naturally only in tracer amounts within uranium minerals.

Since ^{239}Pu does not exist in any larger concentrations naturally it has to be produced. This is done by bombardment of ^{238}U with neutrons in a reactor.

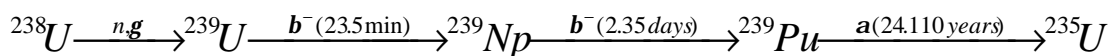


Figure 1: Production and decay of ^{239}Pu .

Heavier Pu-isotopes are produced in the same way (by neutron capture). For example are ^{240}Pu formed when ^{239}Pu are bombarded with neutrons. This means that the longer the ^{238}U is neutron-irradiated, the higher are the production degree of heavier plutonium isotopes. When weapon plutonium is produced, the irradiation is optimised so that

Pu-grade	^{240}Pu mass content
Super grade	2-3%
Weapon grade	< 7 %
Fuel grade	7-19 %
Reactor grade	>19 %

Table 2: Plutonium grades (IPPNW and IEER, 1995)

the fraction of ^{240}Pu (and heavier isotopes) is kept as low as possible. The most common way to grade the Plutonium is according to the ^{240}Pu mass content (table 2). The plutonium used in weapons is in metallic form and the least amount needed is in the 3 to 5 kilogram range (IPPNW and IEER, 1995).

With the help of media plutonium has been given a false reputation of being a more dangerous substance than it actually is (Sutcliffe et al., 1995). The nuclide can enter the body by inhalation, ingestion or through open wounds. Ingestion is not a significant hazard since the gastro-intestinal tract absorbs the plutonium very poor; only about 0.1 % of the plutonium is absorbed. Also, the element is normally not present in high concentrations in human food, since plutonium is poorly spread in the food chain. At inhalation on the other hand about 25 % of the plutonium is absorbed into the blood stream, via the lungs. Plutonium concentrates especially in the liver and bones where it causes long-term radiation. As inhalation is of greatest concern, the size of the particles on which plutonium is connected to is of importance. The radiation effect is of greater concern than the chemical toxicity. (Sutcliffe et al., 1995)

It wasn't until the intensive testing of nuclear weapons took place in 1954 to 1958, and again in 1961 to 1962 that plutonium got distributed in the environment globally. About 10 PBq of $^{239,240}\text{Pu}$ was injected in the atmosphere and plutonium can now be found in most environments (fresh and seawaters, sediments, aerosol particles, inland ice, groundwater etc.) (Pentreath, 1995). Most bomb tests was conducted on the Northern Hemisphere, which have led to that plutonium concentrations generally are higher here than on the Southern Hemisphere. Another important worldwide source of plutonium was the burn-up of SNAP 9A over the Mozambique Channel in April 1964. The U.S. satellite contained plutonium metal, primarily as ^{238}Pu . The ratio of ^{238}Pu to that of $^{239/240}\text{Pu}$ is therefore higher in the Southern Hemisphere than in the northern, and the ratio changes with time because of decay and mixing processes. Apart from the relatively uniform releases from nuclear explosions, other releases, like marine discharges from waste reprocessing facilities, has given enhanced concentrations of plutonium in local or regional environment (Fifield et al., 1996).

After these releases it was realised that the Plutonium isotopes could be used as tracers of environmental processes together with other nuclides of both natural and artificial origin. By identifying ratios for two or more radionuclides one can map the different sources. The ratios can be expressed either as activity ratios or as atom ratios. It does not necessary have to be isotopes of the same nuclides that are compared, non-isotopic elements with similar environmental behaviour can be used as well. It can be hard to find out how much is released from a certain source, like a nuclear accident or a nuclear weapon test, since it already exist radioactive isotopes in the environment, and estimations are usually necessary. Processes like remobilisation and colloidal transport as well as matters like "hot particles" and bio-concentration makes the Pu-distribution a complicated matter (McAninch et al., 1999). In table 3 some, for plutonium (and ^{237}Np), commonly used ratios for source identifications are given for a number of sources. It should be noted that the ratios in the table are as of 1 January 1995.

To be able to get the $^{240}\text{Pu}/^{239}\text{Pu}$ ratio when alpha counting, the energy resolution for the detector has to be good enough to make separation of the two alpha peaks possible. Therefore detection methods like AMS, which do not depend on the energy of the ionising particles, can give this information while conventional alpha spectrometry usually cannot (McAninch et al., 1999).

Source and means of release	Atom ratios ($\pm 1\sigma$ uncertainty)				
	$^{238}\text{Pu}/^{239}\text{Pu}$	$^{240}\text{Pu}/^{239}\text{Pu}$	$^{241}\text{Pu}/^{239}\text{Pu}$	$^{242}\text{Pu}/^{239}\text{Pu}$	$^{237}\text{Np}/^{239}\text{Pu}$
Northern Hemisphere stratospheric fallout from atmospheric weapons testing, of primarily high yield devices ^a	0.000177 ± 0.000032^b	0.1808 ± 0.0057	0.00264 ± 0.00020^c	0.0040 ± 0.0003	0.45^d
Semipalatinsk 21 and Novaya Zemlya, atmospheric weapons testing of low-yield (< 100 kt) devices ^e	0.000157 ± 0.000012	0.0438 ± 0.0001	0.000499 ± 0.000008	0.0000789 ± 0.0000026	0.0208 ± 0.0013
Kyshtym, ^f accidental release, 1957, weapons grade Pu produced in natural uranium graphite-moderated reactors	$0.0000334 \pm 0.0000089^f$	0.0282 ± 0.0001	0.000231 ± 0.000006	0.0000715 ± 0.0000026	0.0727 ± 0.0029
Sellafield, direct ocean discharge of waste from plutonium re-processing activities, weighted over the operating history of the plant up to 1995 ^g	0.00118	0.1838	0.0116	0.0053	1.69
Mike Test (Eniwetok Atoll), ^h near field, tropospheric fallout from testing of low yield device	0.000055^i	0.363 ± 0.004	0.0051 ± 0.0007	0.0194 ± 0.003	—
Bravo Test (Bikini Atoll), ^j near field, tropospheric fallout from atmospheric test	$0.00000791 \pm 0.00000092$	0.32 ± 0.03	0.0038 ± 0.0002	—	0.42 ± 0.04
Chernobyl accident, ^k release of reactor core material that had been subjected to lengthy irradiation, consistent with power production rather than weapons production	0.00334	0.563	0.140	0.0429	0.0228

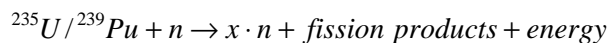
^aKrey et al. (1976; data from Nevada, Utah, and Burbank, CA, show regional, Nevada Test Site fallout and are excluded from the calculated average).
^bCalculated from the data of Hardy et al. (1973) using a $^{240}\text{Pu}/^{239}\text{Pu}$ atom ratio = 0.18.
^cDecay-corrected to 1 January 1995.
^dBeasley et al. (1998a). Sellafield data represents the decay-corrected (1 January 1995), discharge-weighted means for the years 1966–1985 and affects only $^{238}\text{Pu}/^{239}\text{Pu}$ and $^{241}\text{Pu}/^{239}\text{Pu}$ atom ratios.
^eBeasley et al. (1998b).
^fCalculated from the data of Aarkrog (1995).
^gKershaw et al. (1990; 1995).
^hDiamond et al. (1960).
ⁱCalculated from the compilation of Perkins and Thomas (1980).
^jYamamoto et al. (1996).
^kKirchner and Noack (1988).

Table 3 : Plutonium ratios for some important sources (Cooper, 2000)

Nuclear bombs

Fission bombs

The idea behind fission explosives is that some fissile isotopes, like ^{239}Pu and ^{235}U , have a “critical mass”. If the mass of these isotopes exceeds this critical mass, a self-sufficient chain reaction takes place. The critical mass is not a fixed number but depends on the density to which the material is compressed, the presence of neutron flux effecting gadgets (such as moderators and reflectors) and the chemical form and the shape of the fissile material (IPPNW and IEER, 1995). The reaction that takes place can be described with this general scheme:



The experimental value of x are 2.42 and 2.86 for ^{235}U and ^{239}Pu respective, for thermal neutrons (Krane, 1988), and between 2.5 and 3 in fast fission (IAEA, 1998). The fission is most likely to result in two fragments with mass numbers near 95 and 140 (IAEA, 1998). An exponential increase in energy is released in this chain reaction that makes the fuel blow apart and therefore, the reaction to stop. The fission bombs are constructed so that the fissile material becomes critical quickly enough for the desirable explosion effect to be produced, before the fuel itself is blown apart into fragments. This can be accomplished if a plug is cut out of a sphere of pure ^{235}U (the plug and the sphere together makes a critical mass), and this plug later is shot in to the centre of the sphere causing a chain reaction to begin at the moment the critical mass is achieved. The bomb dropped on Hiroshima in Japan was of this type. The Nagasaki-bomb was of different construction. Here the fission fuel, ^{239}Pu in this case, was compressed into the critical stage by conventional explosives. This type is called “Implosion bomb” and its design is the most common in more modern fission devices. Both designs have an initiator, that provides neutrons to initiate the reaction, and usually a tamper, made of ^{238}U , which surrounds the fission material and reflects neutrons back in to the core. The tamper also provides some additional neutrons through fast fission of ^{238}U (Krane, 1988).

Thermonuclear explosives

With an explosive energy release of 2 to 3 order of magnitudes higher than that of the older fission bombs, the thermonuclear explosives took over, soon after it's completion, as the main nuclear weapon in the strategic arsenal both in the U.S. and in the USSR. Fusion reactions have energy criteria, and not critical mass criteria like the fission reactions mentioned above. The energy needed to overcome the repulsive forces between the nucleons and start the fusion process is so high that the only presently known practical way to produce such high energy here on earth is by fission explosions (Draganic' et al., 1989). Fig 2 shows a schematic figure of a thermonuclear explosive. At the detonation of a thermonuclear device a fission-fusion- or a fission-fusion-fission-process takes place. The first fission explosion is an initiator for the forthcoming fusion reaction. This “initiator” is constructed like an implosion bomb (see above), where the

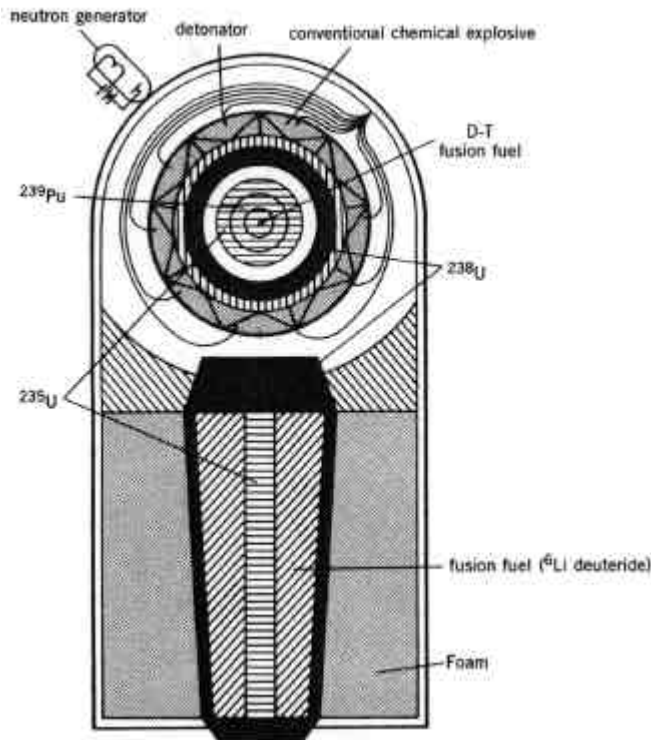
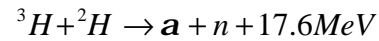
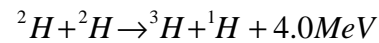
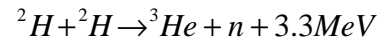
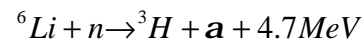


Figure 2: Schematic figure of a thermonuclear explosive

neutrons released at the fusion reaction have high enough energy to cause fast fission in ^{238}U . It is therefore common to enclose the fusion fuel in ^{238}U , and usually about 50% of the total yield come from this last fission reaction in the tamper. (Krane, 1988)

fuel usually consists of both ^{239}Pu and ^{235}U . A small amount of fusion fuel in the centre of the sphere boosts the explosion. The X- and γ -rays produced in this fission reaction heats the fusion fuel as well as it compresses it. As fusion fuel, lithiumdeuteride, $^6\text{Li}^2\text{H}$ (sometimes $^7\text{Li}^2\text{H}$) is used. Some of the reactions that starts ones the ignition temperature for the fusion fuel is reached are the following four:



Since the main energy source in the thermonuclear explosions is fusion involving ^2H and ^3H the name Hydrogen bomb or simply H-bomb is commonly used. The fast

Post detonation of nuclear bombs

The environmental consequences of an atmospheric nuclear detonation depend to a large extent on the construction of the bomb and on the location of the detonation. The more fission that takes places – the more fission fragments, like ^{137}Cs , ^{131}I and ^{90}Sr , are produced. Therefore the presence of a tamper elevates not only the yield but also the amount of fission fragments. Radioactive fallout material is a mixture of fission fragments, fissile material that never underwent fission (unspent nuclear fuel) and activated substances that was present in the vicinity of the detonation (for example soil, water, air and metallic constructions) (Noshkin et al., 1997a). A number of radioactive elements are also produced due to decay of these radionuclides.

The time the isotopes stay in the atmosphere depend among other things on the size of the particles they are connected to. Heavy fragments fall back to earth in the extreme vicinity of the detonation within minutes after the explosion, while less massive particles stays a longer time in the air and are therefore more affected by the wind. Particles that are born downwind and fall to the earth's surface within several hours after detonation are

designated local fallout. The nature of the fallout depends to a large extent on the strength of the explosion and the altitude of the detonation. If the detonation is powerful enough, or detonated at a high altitude, the bomb debris can reach the stratosphere where it is affected by stratospheric winds. Vertical mixing in the Polar Regions in the winter and early spring can bring the radionuclides down to the troposphere from where it can fallout with rain or as direct deposit. The radioisotopes can be present in the atmosphere for years before they fallout on any place on earth. This is called global fallout.

Nuclear bomb testing in the Marshall Islands

The history of the Marshall Islands as a nuclear weapons test area

Marshall Islands are located in the Pacific Ocean at between 4° and 19° North latitude, and 160° and 175° East longitude (fig. 3). The capital of these tropical atolls and islands, Majuro Atoll, is home to roughly half the country's population of 60,000. The total land area of the Marshall Islands is about 180 square kilometres, which is only 1.5% of the total area of the country.



Figure 3: The location of the Marshall Islands on the globe

In June 1946, the first post World War II test series, Operation Crossroads, was performed by U.S.A. at the Bikini atoll in Marshall Islands. This was only about a year after the first nuclear bomb test ever took place at operation Trinity at Alamogordo, New Mexico, U.S.A. In July 1947 the Marshall Islands and the rest of Micronesia became a United Nations strategic Trust Territory administered by the United States. Marshall Islands (known as the western part of the Pacific Proving Grounds (PPG)) and some other Pacific Islands were together with Nevada Test Site (NTS, originally called the Nevada Proving Grounds or NPG) the main U.S. test sites during the time period 1946 - 1958. Most tests on Marshall Islands were conducted on barges over the lagoons or the reefs, and the two atolls used were Enewetak and Bikini. Even though the number of tests conducted here, 66, only represents about 14 % of all U.S. tests, they account for nearly 80 % of the total yield from U.S. atmospheric detonations and about 20% of the estimated total yield from all atmospheric nuclear testing. A little more than 50% of the yield from tests conducted on the Marshall Islands is estimated to have come from fission (Robison and Noshkin, 1998).

The Castle Bravo incident

Operation Castle is the code name of a series of high yield thermonuclear weapon design tests that took place at the Bikini atoll in the first half of 1954. A number of new concepts were tested at operation Castle, and the expected yields were exceeded by far. Three out

of the six tests had an explosive yield exceeding the equivalent of 10 Mega Ton (Mt) of TNT explosives, which is about 700 times the strength of the Hiroshima bomb. The one with highest yield, Castle Bravo, is with its 15 Mt the largest nuclear bomb ever detonated by the U.S.A. (the expected yield was between 4 and 8 Mt). Castle Bravo was detonated on a platform about two metres over the corral in the NW corner of the Bikini Atoll, at 6.45 AM on 1 March local time (Simon and Robison, 1997a). Bravo was the first "dry", or solid fuelled, thermonuclear bomb tested by the U.S.A., and the fuel consisted of enriched ${}^6\text{Li}$ -deuteride (${}^6\text{Li}^2\text{H}$). It was built with a ${}^{238}\text{U}$ tamper designed to increase the explosive power a lot, and 2/3 (10 Mt) of the yield resulted from fast fission in the tamper. The crater that this surface-detonated bomb left measures 73 m in depth and has a radius of 912 m (Noshkin et al. 1997b). The top of the cloud from the detonation reached an altitude of about 40 km, and reached therefore far into the stratosphere.

The normal wind condition at the area of detonation is a prevailing NE trade wind (coming from NE), but only seven hours before the detonation of Bravo there were indications that the weather conditions were getting less favourable with winds at an altitude of 6,000 meters heading E and NE towards Rongelap. This together with the higher than expected yield, led to the contamination of four inhabited atolls, Rongelap, Rongerik, Ailinginae and Utirik (fig. 4), with fallout from the Bravo detonation. The

Japanese fishing boat Fukuryu Maru, or Lucky Dragon, located about 150 km east of Bikini was also contaminated with Bravo fallout.

Despite the hope-giving name of the vessel, all 23 crewmembers suffered from radiation sickness, and one member later died of liver and blood damages (Simon, 1997, Eisenbud, 1997).

6 hours after the Bravo test Air weather service personnel situated on

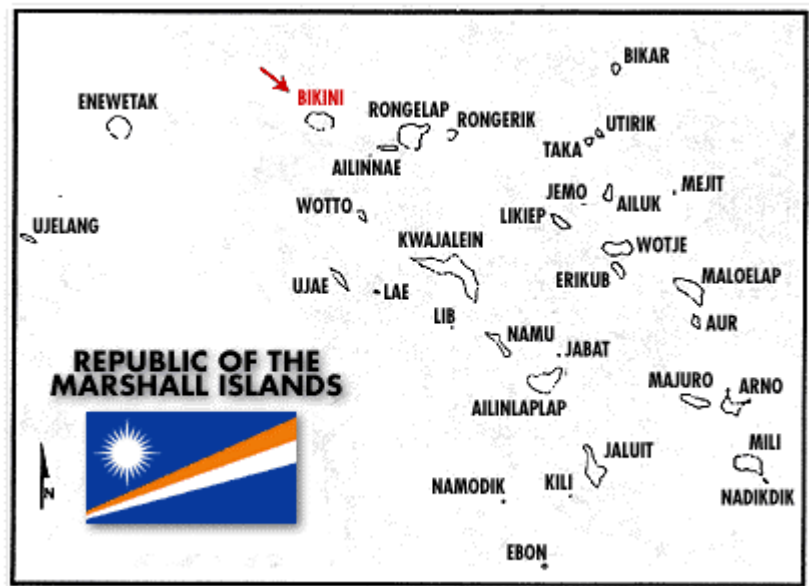


Figure 4 : The Marshall Islands

Rongerik, about 300 km east of Bikini, found their gamma monitors to peak

at their limit value of 1 mSv h^{-1} (Cronkite et al., 1997). The 28 Air weather service personnel were evacuated about 24 hours after the on-set of fallout and they had then received an external whole-body dose estimated to be 0.78 Gy (Eisenbud, 1997). People on the Rongelap atoll and the Ailinginae atoll were evacuated about 50 hours after the Bravo fallout reached Rongelap, on 3 March. People on the Utirik atoll were evacuated on 4 March (Simon, 1997). Estimation on the mean whole-body external dose to persons on

Rongelap is 1.75 Gy. Luckily people were situated in the SE corner of the atoll while the plume from Bravo went over the less populated NW part of the atoll. If the people had lived in the NW instead, the mean dose would have been about 8 Gy (Donaldson et al., 1997).

In August 1958, the United States ended the program of nuclear testing in the Marshall Islands, and since November 1962 all nuclear tests conducted by the United States has been underground, and most of them have been conducted at the NTS (Donaldson et al., 1997). The Republic of Marshall Islands became independent in 1986, and joined the United Nations in 1991.

Accelerator Mass Spectrometry (AMS) for Plutonium Measurements

History

In some of the first measurements of plutonium, Geiger counters, proportional counters or ionising chambers were used. The first semi-conductor detectors came in the late 40's. These were further developed in the 50's and in the end of that decade α -spectrometric techniques were widely used. The development continued, and in the 60's, reliable multi-channel analysers became available (Pentreath, 1995). Long-lived isotopes are very time-consuming to measure by conventional decay counting. This can be overcome if one instead of measuring the decays of the atoms measures the number of atoms or something proportional to this. This is done in AMS as well as in a number of other measurement techniques, like for example Inductively Coupled Plasma Mass Spectrometry (ICP-MS) and Resonance Ionisation Mass Spectrometry (RIMS). As the names of these techniques tell, mass spectrometry is used as part of the detection system. It should be noted that other sensitive methods that do not have mass spectrometry as a part of the system, like Fission Track Analysis (FTA), exists as well.

AMS have mainly been developed in the forth quarter of the 20:th century, but as early as 1939 was the first time an accelerator was used for isotope identification. Alvarez and Cornog conducted the experiment, where a cyclotron was used to detect ^3He and ^3H . AMS was reintroduced almost 40 years later, in 1977, when a man named Muller also experimented with the use of cyclotrons for ^3H detection. Later that year two different groups reported successful ^{14}C -observations from natural materials with the use of tandem accelerators (Fifield, 1999). Today it is almost exclusively tandem accelerators that are used in AMS. Although a number of tandem accelerators have been built exclusively for AMS, the demand of more powerful accelerators for nuclear research, has left a lot of "used" accelerators that have been modified to become, or partly become, AMS facilities.

Applications for AMS

The main AMS-application is measurements of ^{14}C –abundance for "carbon dating", but a number of other stable and long-lived nuclides, such as ^{10}Be , ^{36}Cl , ^{26}Al and ^{41}Ca , are also measured. The isotope of interest is usually counted in relation to a stable isotope of the same nuclide. Isotopic sensitivities (the rare to stable isotope ratio) for these isotopes can be as low as 10^{-15} and the detection limit $\sim 10^5$ atoms (Hotchkis et al., 2000).

Progress in measuring man-made long-lived radionuclides such as certain actinides (^{236}U , ^{237}Np , ^{239}Pu) and fission products (^{90}Sr , ^{99}Tc , ^{129}I) using AMS have been seen in the 90:s, and very high sensitivities can be accomplished. Since many of these isotopes have a long half-life and since the abundance usually is low in environmental samples, AMS is to prefer over conventional alpha spectrometry for such measurements (McAninch et al., 1999).

A group in Toronto, Canada reported the first AMS detections of ^{244}Pu and ^{236}U . ^{236}U are used as a neutron flux monitor in safeguard systems of nuclear power plants. The $^{236}\text{U}/^{235}\text{U}$ ratio gives valuable information about nuclear fuel that has been in a reactor.

Much development of AMS techniques for measurements of long-lived plutonium isotopes and ^{237}Np has been made in Canberra, where groups from the Australian National University (ANU) and from the University of Manchester have conducted experiments. Plutonium isotopes are in the year 2000, routinely measured there. Other laboratories, like LLNL, Ansto and laboratories at Munich, are establishing capabilities for plutonium measurements (Fifield, 2000). The performances of AMS facilities vary from one to the other and many laboratories have specialised in measuring only one or a few isotopes. New systems for high precision ^{14}C dating based on small accelerators with voltages as low as 0.5 MV are probably the best example of such isotope-specialised developments (Fifield, 2000).

Important steps in AMS

Since the tandem accelerator is the far-most common type of accelerators used for AMS, only this type will be discussed here. Under "General" I go through the principal steps in a tandem accelerator, as it usually is equipped for plutonium measurements. It should however be understood that this is not exactly how every AMS facility looks in detail, but instead a brief overlook of the most important steps in the tandem accelerator. How the tandem accelerator at LLNL is equipped for plutonium measurements is described under "At LLNL". Figure 5 shows the AMS line for Pu-measurements at LLNL.

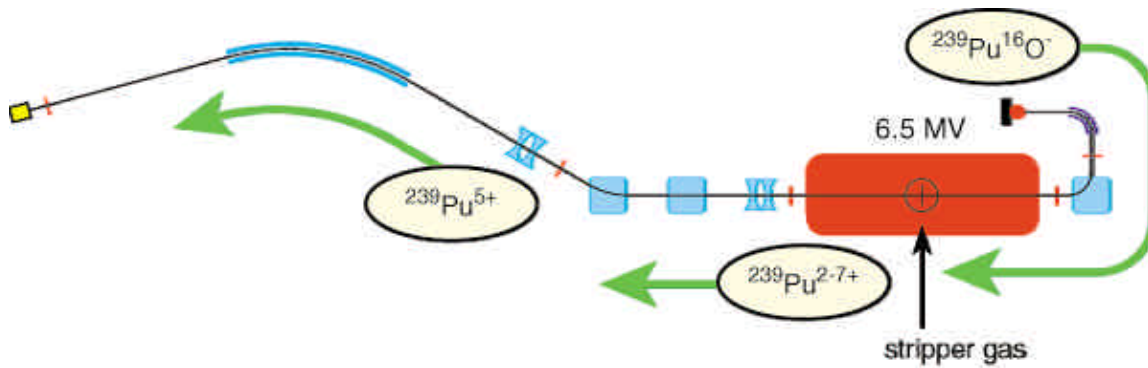


Figure 5: The AMS line for Pu measurements at LLNL.

Ion source

General: The ion source is one of the most important and complex parts of the accelerator system. In tandem accelerators one has to use a negative ion source, which is obvious considering the way the accelerator itself works (see "Tandem electrostatic accelerator" below). A "bonus" that comes with the use of a negative ion source at the detection of certain elements, like for example C, is that interfering elements (N in the case of C-detection) do not form stable negative ions. Usually a Cs-sputter ion source is used. Here the target (the sample) is bombarded with positive Cs ions - a process that enhances the formation of negative ions. The majority of the sample forms neutral ions during the sputter process. These simply bounce around in the ion source and vacuum system until they get stuck to something. Automated sample changing system and multiple sample holders (cassettes) increase the throughput of the system.

At LLNL: A Cs-sputter ion source was used. The sample wheels used at LLNL could hold 64 samples.

Low energy mass analysis

General: The basic idea behind mass spectrometry is that the Lorentz force, which affects charged particles in motion in a magnetic field (with a velocity component perpendicular to the field) act as a radial force on the particle, and is hence depending on the particle's mass. To see how the radius is depending on the mass we start out with the Lorentz equations:

$$\begin{cases} \vec{F} = \frac{d}{dt}(\vec{g}m_0\vec{n}) = q(\vec{E} + \vec{n} \times \vec{B}) \\ \frac{d}{dt}(\vec{g}m_0c^2) = q\vec{g}\vec{E} \end{cases}$$

Equation 1 : The Lorentz Equations

The first equation gives the force on the particle and the second equation the change in energy of the particle. If the magnet field is kept constant in time, no electrical field will be induced and the Lorentz equation can be written as:

$$\begin{cases} \vec{F} = q(\vec{n} \times \vec{B}) \\ \frac{d}{dt}(gm_0c^2) = 0 \end{cases}$$

Equation 2 : The Lorentz equations without any electrical field present

In classical mechanics the radial force on a particle moving in a circular path with radius "r" with constant speed is given by:

$$F = \frac{m\mathbf{n}^2}{r}$$

Equation 3: The Radial force

If the particle is moving perpendicular to the magnetic field, the combination of eq. 2 and eq. 3 gives:

$$r = \frac{m\mathbf{n}}{qB}$$

Equation 4: The radius, r, of a particle with the mass, m, and charge, q, moving perpendicular to the magnetic field, B with the velocity, v.

Accordingly, all equally charged particles move in a circular path in the magnetic field, B, with a radius "r" that depends on p = m·v.

The negative ions that leave the ion source are accelerated towards a bending magnet. Here, in the magnetic field B, all the like-charged ions with the same "p" are moving in a circular path with radius "r" according to equation 4. Even though the ions are accelerated by the same electric field, some do get a little more or a little less energy. These energy-tails can cause interference to appear from neighbouring masses, and it is therefore common to add an electrostatic analyser (ESA). This instrument, which is used to select ions with the correct energy, is placed in-between the ion source and the spectrometer (the bending magnet). Beam line parameters commonly used for AMS are the magnetic and electrostatic rigidity, χ_B and χ_E , respective. These are defined according to equation 5 and 6 below.

$$\chi_B = rB = p/q$$

Equation 5: Magnetic rigidity

$$\chi_E = rE = pv/q$$

Equation 6: Electrostatic rigidity

The vast majority of the negative ions, which are formed, cannot make it around the low energy-bending magnet and the electrostatic analyser, because they have the wrong rigidities.

At LLNL: A recent upgrade for improved capabilities of heavy element - measurements included the installation of a 90-degree electrostatic analyser placed in-between the ion source and the bending magnet. The two analysing instruments bend the beam 90 degrees each (McAninch et al., 1999).

Tandem electrostatic accelerator

General: The ions are accelerated towards the stripper in a static electric field with a potential in the mega volt (MV) – range. The accelerator has to be situated in an insulating gas filled tank to prevent arcing to occur at such high voltages. The gas used is usually SF₆ at pressures between 2 and 7 bars. The high voltage can be produced in two different ways. In a Van de Graff tandem accelerator a fast moving rubber belt collect positive charge from a voltage supply and carry these to the high voltage terminal. If the belt is replaced with a chain system, the accelerator is called a “Pelletron”. The charge transport is a process with a rather long response time, and when fluctuations in the voltage has to be stabilized, a corona discharge from the voltage terminal to the tank wall. The other way to produce a high potential difference in the accelerator is to use RF signals.

The stripper can be either a carbon foil or a gas, but the principle is the same; the gas or the foil “strips” the negative ions on a number of electrons, leaving the ions positively charged on the other side of the stripper. The stripper also breaks up accelerated molecular ions. Now a second acceleration of the particles takes place (hence the name “tandem accelerator”). The sought-after nuclide does not come out in one specific charged state, but instead a spectrum of charged states is found. Unfortunately only one of the states can be chosen for measurement. The stripper gas, O₂ or Ar in most cases, are re-circulated to a large extent while the foil gets destroyed by the radiation damage and has to be changed often.

At LLNL: The tandem is rated to +10 MV, and for Pu it is run at +6.5 MV. The insulating gas is SF₆ at about 7 bars. Gas stripping is used with argon gas.

High energy analysis

General: After acceleration the ion beam is analysed in a second mass spectrometer. By switching the magnetic field during the run, different masses of interest can be analysed. The beam line is this way scanned so that information about a number of isotopes is gathered. The measuring time for each isotope depends on the abundance of the elements with the specific rigidity. Often there is also an electrostatic analyser or a Wien filter in the high-energy end of the AMS system. The Wien filter consists of an electric field and a magnetic field perpendicular to each other (fig. 6).

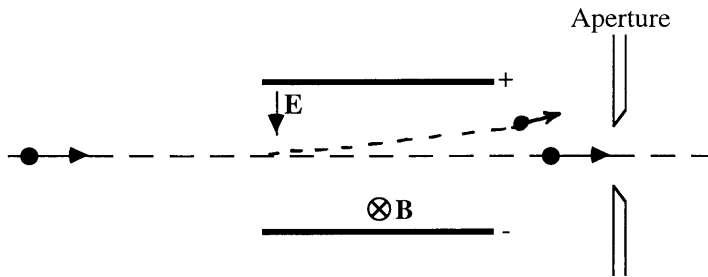


Figure 6 : The principal of a Wien filter. (The picture is taken from chapter 3: Beam Transport (By K. Stenström) from unpublished literature for an accelerator course given by R. Hellborg, at the Department of Physics at Lund University year 2000).

Only if $qE = qvB$ can the particle continue undeflected. That means that the Wien filter is a velocity filter.

At LLNL: The accelerator at LLNL has recently been upgraded for better performances in measurements of heavier elements (200-250 amu) like actinides. The main hardware upgrade is a heavy element beamline including a high energy Electrostatic Analyser (ESA). The ESA deflect the beam 45° with a radius of 4.4 m. The bending magnet bends the beam 30 degrees. (McAninch et al., 1999)

Detector

General: The detector, a solid-state detector or a gas counter, makes the end of the AMS system. Here a signal proportional to the total energy of the incoming particles is measured. The detector system is usually constructed so that the specific energy loss, dE/dx , of the ions can be measured. This gives additional information on the atomic numbers of the detected ions. An extra mass determination, especially efficient for heavier ions, can be performed if a time-of-flight detector is used together with the ordinary detector. Here very precise velocity information is given as the ions flight path is measured over 1-3 m, with a high time resolution.

At LLNL: The detector is a gas-filled ionisation detector. The gas consists of 90% Ar and 10% methane, and the pressure is about 11 kPa. As entrance foil a thin piece of aluminised Mylar is used. The ionisation from the slowing-down of the ions is measured as a charge signal. This is amplified to a voltage signal and then digitised.

Other

Apart from the instruments described above a number of steerers, lenses and slits etc. are included in the AMS system. I will however not treat these in this report.

Preparations and performances for plutonium measurements with AMS

Sample preparation

The samples are prepared as a solid matrix with a metallic carrier used at the precipitation step at the chemical preparation. The carrier used for Pu-samples prepared for AMS at Lawrence Livermore N.L. was iron (Fe). Here 1 mg niobium (Nb) was also added to the sample and the mixture was packed in a sample holder. Nb and Fe are present approximately as 1:1 by mass. The Nb work as a matrix enhancer, which improves the PuO^- output and production efficiency. It also makes the sample somewhat more refractory and works to improve the thermal stability. As a substitute for a stable isotope for comparison with the long-lived actinide isotope of interest an isotope dilution spike, ^{242}Pu , is added at the preparation of the sample.

Tuning

Plutonium has no stable isotope, and therefore, no macroscopic beam available for setting up the beam line and adjusting the ion source for optimum output. Uranium and thorium can be used for this purpose as a surrogate. Uranium is with its chemical and mass likeliness to plutonium preferable to use for studying the ion source. Thorium on the other hand can be used to tune the beam transport as this avoids uranium contamination of the ion source (Fifield et al., 1996). At LLNL Niobium (Nb) is used for tuning the accelerator. This is convenient since Nb is used in every sample. Only what magnet settings to use for plutonium is given and not any information regarding ionisation efficiency and count rate. For these purposes plutonium is used.

Efficiency

The overall efficiency of a system is the number of atoms detected divided by the number of atoms in the sample for a specific isotope, and it is the product of:

1. Fraction of the sample used.
2. Efficiency for producing negative ions.
3. Yield for the selected charge state.
4. Transmission efficiency.
5. Detection efficiency.

It is no. 2 and 3 in the list above that is the main efficiency reducing steps of an AMS system. Which charge state that is selected for analysis depends not only on the yield but also on other system limitations and on the possibility of molecular interference for some charge states. The high-energy spectrometer at LLNL is set to analyse Pu^{5+} ions, which have an energy of 38.6 MeV when they leave the accelerator, and for which the stripping efficiency is ~5-10%.

The efficiency for producing negative ions in the ion source vary with the electron affinities of the elements, and molecules are often more efficient in forming negative ions, than single atoms are (Hotchkis et al., 2000). The efficiency for conversion of Pu atoms to PuO^- ions at the accelerator in Livermore is ~ 0.3% if a sample is run to the end,

and ~ 0.01% for a 3 minutes run. This is the main “efficiency-reducing” step in the system. The transmission for the rest of this accelerator system, excluding the stripping, adds up to ~ 70 % (efficiencies are; low energy spectrometer, ~75%; transmission through the tandem and high-energy spectrometer, ~95%; detector efficiency, essentially 100%). The detector is usually set to accept only about 80% of the counts for reduction of interference.

For a ~3 min Pu-measurement, the overall efficiency is $2 \cdot 10^{-6}$ to $1 \cdot 10^{-5}$ (i.e. 2-10 measured counts for 1 million atoms of ^{239}Pu in the original sample). The overall efficiency for long-lived radionuclides is $10^6 - 10^9$ times higher (up to 10^8 times higher for the longest-lived plutonium isotope, ^{244}Pu (Fifield et al., 1996)) in AMS compared to that of decay counting, and the sample sizes and/or measurement time can thereby be reduced accordingly (Hotchkis et al., 2000 and McAninch et al., 1999).

Detection limits

The present detection limit for plutonium with AMS is $\sim 10^6$ atoms (~ 0.5 fg). This is for ^{239}Pu at least two orders of magnitude lower than that by alpha spectrometry (Fifield et al., 1996). This low detection limit makes it for example possible to use ^{244}Pu as a tracer in experiments using human subjects (Fifield, 2000). The ultimate detection limit for actinides at LLNL is expected to be $\sim 10^5$ atoms (McAninch et al., 1999). At present it is $\sim 1 \cdot 10^6$ atoms per sample for ^{239}Pu , and $0.3\text{-}0.6 \cdot 10^6$ atoms per sample for ^{240}Pu and ^{241}Pu .

Background levels

Detection of very low isotope ratios is possible with AMS due to its way of suppressing backgrounds from adjacent stable isotopes, isobars and equal-mass molecules. The total background consists of two parts, misidentification in the detector system and contamination of the isotopes of interest (Hotchkis et al., 2000). Interference from other actinide isotopes, principally ^{238}U , are more serious than interference from lighter isotopes because they can not as easy be distinguished in the detector from the actinide of interest on the basis of their energy (Fifield et al., 1996). Apart from sample-contamination with Pu, two sources of interference are of main concern at the AMS at Lawrence Livermore laboratory; interference from Uranium and from Platinum in samples with high concentrations of these elements. At the AMS system at LLNL, ^{239}Pu are injected as $^{239}\text{Pu}^{16}\text{O}^-$. ^{238}U interference occurs then as the isobar $^{238}\text{U}^{17}\text{O}^-$ or as energy tailing of the more abundant $^{238}\text{U}^{16}\text{O}^-$ (McAninch et al., 1999). The routinely measured plutonium isotopes have no stable isobars, and this makes the detection simpler than for example detection of ^{99}Tc , where interference from ^{99}Ru has to be taken into account. Contamination can have its origin either from the laboratory or from the ion source. In the laboratory, where the sample is prepared in a series of chemical procedures, contamination of reagents and tracers as well as background plutonium can be present. The ion source can be contaminated after running relatively “hot” samples and cause a higher than normal background levels for the system. These “memory effects” makes the order of running a set of samples crucial and sets an upper limit for what activities that can be measured with the AMS (Fifield et al., 1996).

Precision

An AMS system's precision depends on its stability. A stable system shows little spread of a value at repeat measurements of a sample (it has good reproducibility), and the limiting factor is then principally the uncertainty from counting the ions in the detector (Hotchkis et al., 2000)

PART 1: Measurement of Plutonium in sediment from the Rongelap Atoll using AMS.

Background

When the plume from the Bravo detonation reached the Rongelap Atoll, part of the material was deposited as close-in fallout on the islands and lagoon of Rongelap. Contribution of fallout to Rongelap from other tests conducted 1956 and 1958 was less than 1% of the Bravo fallout (Noshkin et al., 1998). Some of the Bravo fallout-material that dispersed in the lagoon rapidly settled to the bottom surface sediments while some were dissolved in the water, and eventually discharged into the Pacific Ocean (Robison and Noshkin, 1998). Many of the deposited radionuclides have such short half-life that they are now present in very low levels. Other radionuclides, like ^{239}Pu , have barely disintegrated at all, due to their long half-lives. Though, other processes, physical, biological and chemical, remobilise the radionuclides. These processes may change the concentrations, distributions and/or inventories of long-lived radionuclides present in the lagoon over time. Fallout on the soil on islands is for example influenced by wind, rain and sorption, while the movement of the water, among other things, influences the radionuclides present in the sediment and the lagoon water. The fallout is mainly deposited as fine material, but processes have made it possible for radionuclides in sediment to also become associated with coarse material ($>0.5\text{mm}$), such as Foraminifera (unicellular organism on the borderline between plants and animals), coral, remains of algae and shells from molluscs (Noshkin et al., 1997b). There is approximately a factor ten in difference in concentration associated with surface sediments from the north compared to samples from the southern part of the Rongelap Atoll. This was also estimated for the gamma dose rates on the northern and southern islands one day after the Bravo test (Noshkin et al. 1998). Regarding soils and vegetation samples, concentrations on the southern islands of Rongelap are about a factor of five lower than those on the northern islands of the atoll (Robison et al., 1997).

In September 1978, during the Northern Marshall Islands Radiological Survey (NMRIS), ten surface (0 – 4 cm) sediment samples were collected on shallow water (1 – 2 meter deep) outside islands in the Rongelap Atoll. This survey and the result for the samples collected here are described in Noshkin et al, 1998. All the samples were analysed for ^{241}Am and eight of them for $^{239,240}\text{Pu}$ as well. Results from this survey are shown in table 4 below.

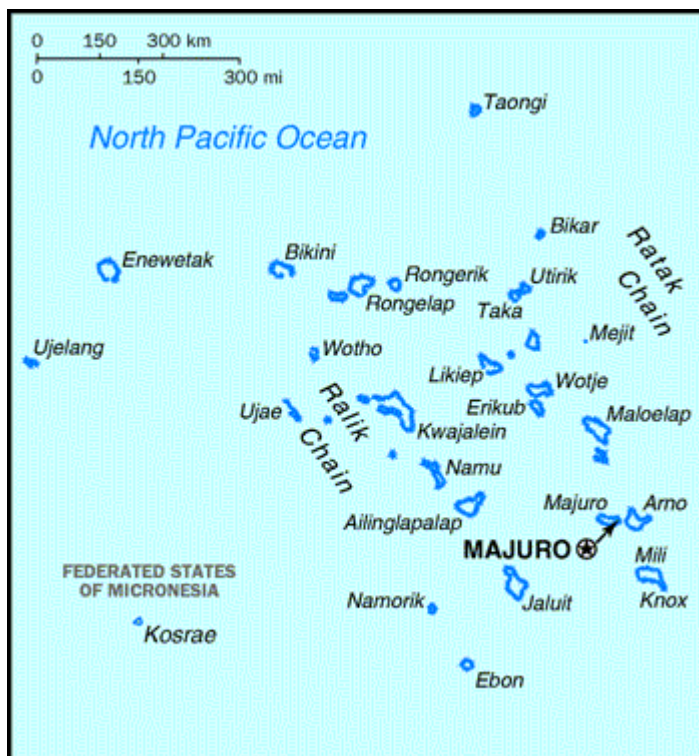
	Results (mean and (range))	As a % of the value for Bikini*	As % of the value for Enewetak*
$^{241}\text{Am} / ^{239,240}\text{Pu}$ activity ratio (1978)	0.67 ± 0.11	--	--
^{241}Am concentration (1978)	6.85 (3.4 – 13.0) Bq kg ⁻¹	--	--
$^{239,240}\text{Pu}$ concentration (1978)	10.6 (4.3 – 19.4) Bq kg ⁻¹	--	--
^{241}Am inventory (1981)	0.63 ± 0.09 TBq	--	--
$^{239,240}\text{Pu}$ inventory (1978 and 1981)	0.94 ± 0.16 TBq	~ 3 %	~ 6 %
$^{239,240}\text{Pu}$ concentration (1978 and 1981)**	--	~ 2 %	~ 5 %

Table 4 : Results from 1978 and 1981 for surface sediment (0 – 4 cm) of the Rongelap Atoll.

*See below for a description of how this comparing is done.

**Calculated from the inventories with some estimations made (see below)

The mean $^{241}\text{Am} / ^{239,240}\text{Pu}$ activity ratio, 0.67 ± 0.11 , is in agreement with the mean ratio from 19 samples collected in Bikini in 1979, 0.69 ± 0.17 (Noshkin et al. 1997a). The $^{241}\text{Am} / ^{239,240}\text{Pu}$ activity ratio changes with time due to ingrowth of ^{241}Am from the decay of ^{241}Pu . The mean ratio as of year 2000 is after decay/ingrowth corrections about 0.72 ± 0.12 in the Rongelap Atoll.



In 1981 surface sediments (0 – 4 cm) were collected throughout the Rongelap lagoon for ^{241}Am analysis, and the results from this survey is also described in Noshkin et al, 1998. The surface (0 – 4 cm) inventory of ^{241}Am in the Rongelap lagoon was estimated from these results, and the surface inventory of $^{239,240}\text{Pu}$ was calculated with the mean $^{241}\text{Am} / ^{239,240}\text{Pu}$ activity ratio factor from 1978 (0.67 ± 0.11) (table 4).

Figure 7 The Marshall Islands

In 44 cores of mean depth 18 ± 6 cm, collected over the years at the Bikini and the Enewetak Atoll, inventories of different radionuclides in the surface sediment (0 – 2 cm) as well as to the total core depth (10 to 30 cm) has been determined in Robison et al., 1997. All radionuclides were well mixed to a depth of 9 cm and below about 10 cm the concentrations decreased with depth. The estimated percentage of how much the surface (0 – 2 cm) inventories represented out of the total inventory (to depths of 10 – 30 cm) was calculated. This ranged from 2 to 25% and averaged $13 \pm 5\%$ for all the measured radionuclides. This value has been used at calculation of the total lagoon inventories and activity per unit area to 30 cm, for all the radionuclides, for Bikini and Enewetak Atoll. These amounts should be seen as lower limits because radionuclides are evident at greater depths (than 30 cm) in some cores from Enewetak. Since the ^{241}Am appears to be reasonably well mixed over at least the first 4 cm in the Bikini and the Enewetak atolls, the inventories to 4 cm in the two atolls are estimated to be twice the inventories to 2 cm. The percentage of the inventory in the top 4 cm are thus about $26 \pm 10\%$ of the total inventory (to depths of 10 – 30 cm) for each radionuclide in the two atolls. The estimated surface (0-4 cm) inventory of $^{239,240}\text{Pu}$ in the Rongelap Atoll from 1981 is about 3% of the value for the Bikini Atoll and about 6% of the value for Enewetak Atoll. The areas of the lagoons in the Rongelap, the Bikini and the Enewetak Atoll are 1025, 629 and 933 km², respective. If we make the estimation that the density of the sediments in the three atolls is the same we can from the inventories above calculate the mean $^{239,240}\text{Pu}$ concentration in the surface (0 – 4 cm) sediment in the Rongelap Atoll to be about 2% and 5% of that of the Bikini Atoll and the Enewetak Atoll, respective.

A way of decreasing the dose rate on the islands of the Rongelap Atoll and the Bikini Atoll is to replace the soil, which on the Marshall Islands consists of calcareous material with a thin overlaying layer of organic matter (Donaldson et al., 1997), with less contaminated material. It has been discussed to use sediment from the Rongelap lagoon for this purpose since it seems to be less contaminated than the soil of the islands in both the atolls (Noshkin et al., 1998).

Between 1990 and 1994 the Republic of Marshall Islands conducted an independent monitoring program that included soil sampling from all the atolls and islands in Marshall Islands (Simon and Graham, 1997). The median $^{239,240}\text{Pu}$ – surface (0 – 5 cm) soil concentration for northern Rongelap was found to be 940 Bq kg⁻¹. This shall be compared to 107, 130, 200 and 83 Bq kg⁻¹ for islands in the southern Rongelap Atoll, in the Bikini Atoll, in the northern Enewetak Atoll and in the southern Enewetak Atoll, respectively. We make the following denotion:

$$Q = \frac{{}^{239,240}\text{Pu concentration in the surface (0 to 5 cm) island soil}}{{}^{239,240}\text{Pu concentration in the surface (0 to 4 cm) lagoon sediments}}$$

Equation 7 : Ratio of $^{239,240}\text{Pu}$ conc. in surface soil to that in surface sediment

This ratio, Q, is higher on Rongelap Atoll than on Bikini Atoll and Enewetak Atoll. If we for Rongelap and Enewetak, where two soil concentrations are given (one for the northern- and one for southern part of the atoll), uses the lower value as a minimum-, and the higher value as a maximum mean $^{239,240}\text{Pu}$ concentration in the surface (0 – 5 cm) island soil, we get a Q for the Rongelap Atoll, which is about 40 to 360 times larger than

that for the Bikini Atoll. Compared to Enewetak, the Q-value for Rongelap is about 10 to 230 times larger. Why do we see this difference in Q? The fact that a number of bomb tests have been conducted on the Bikini and the Enewetak Atolls before and after the Bravo detonation, and that no tests have taken place at the Rongelap Atoll is of course of importance (Donaldson et al., 1997). Even though it is hard to find the reasons for the variations in the Q-values because of the possibility of multiple causes, it is of interest to see if the values mentioned above are correct also for larger depths.

If the vertical distributions of plutonium in the sediment are the same for the three atolls, the reason for this difference in distribution could be that the remobilisation of plutonium to the overlaying lagoon water has been more rapid on Rongelap than what it have been at the two other lagoons. A relatively larger concentration of $^{239,240}\text{Pu}$ in the lagoon water at Rongelap compared to on the Bikini and Enewetak Atolls could be an evidence of this. The plutonium could perhaps however also remobilise from the soil on islands to the lagoon water. In table 5, with data from Robison and Noshkin, 1998, we can see that the $^{239,240}\text{Pu}$ -concentration in lagoon water from Rongelap are 3 % and 6 % of the Bikini and Enewetak concentrations, respective. This is in agreement with the differences in surface sediment concentrations for the three atolls, which indicates that no “extra” plutonium is remobilised from the sediment column at Rongelap compared to the other two atolls.

Whether the vertical distribution of plutonium in the sediments (and/or soils) is different for the atolls or not, is of particular interest if it is decided to use the Rongelap sediment to replace the soils on islands in the Bikini and Rongelap Atolls.

If plutonium is found in larger than expected concentrations at depth at Rongelap, this implies that the sediment here was, somehow, more mixed than sediments on Bikini and Enewetak. Such a mixture could be the result of a more bioactive environment.

Inventories to depths exceeding 4 cm would then of course be larger than if the distribution pattern for Bikini and Enewetak (Robison and Noshkin, 1998) is used.

Location	Sample date	Number of samples	Mean $^{239,240}\text{Pu}$ conc. [Bq m^{-3}] in solution	Total inventory in lagoon water [GBq]
Enewetak Atoll	1972 – 1982	131	0.78	35
Bikini Atoll	1972 – 1982	71	1.54	44
Rongelap Atoll	1978, 1981	17	0.043	--
1 – 5 miles west & south of Bikini (surface water)	1972	5	0,55	--
1 mile south of Wide pass, Enewetak (surface water)	1976	3	0,20	--
North Equatorial Pacific surface water	1972 – 1984	26	0.014	--

Table 5 : Mean concentrations and inventories of $^{239,240}\text{Pu}$ in seawater from the Marshall Islands

Method

Sampling

Since I personally did not participate in the survey when the samples were collected, I will not go into detail about how this was done. Figure 8 shows the sample locations, and further information about the sample stations and the sampled cores can be found in table 6.

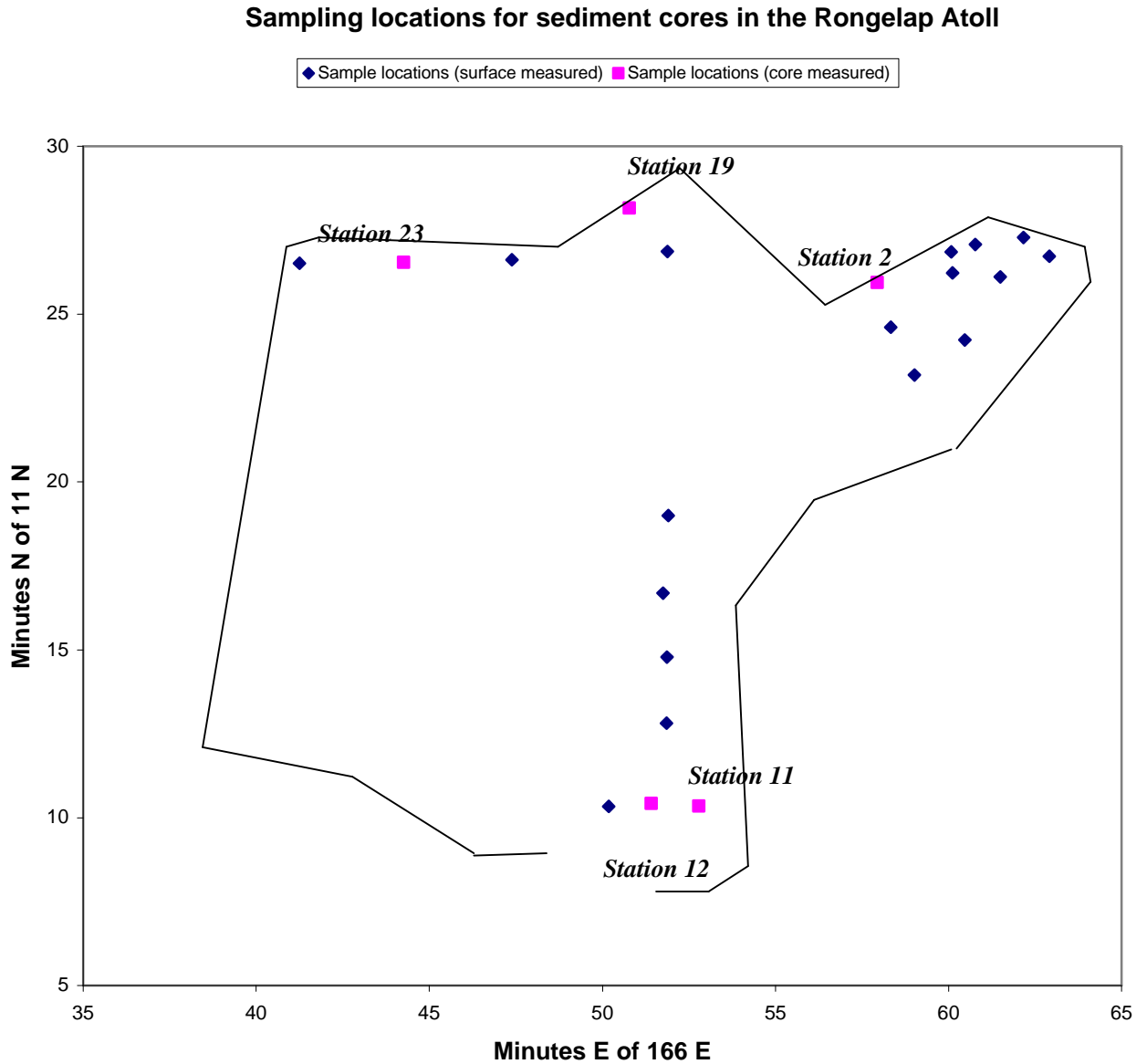


Figure 8: Sediment sample locations

The sediments were oven dried in steel cans and ball milled into a fine powder. The range of the dry/wet- weight ratio is in the range of about 0.5 to 0.8 for the sediment samples analysed.

Station no.	Sampling date	Degree North	Degree East	# of cores	Core depth [cm]
1	1998-10-29	11.45	167.05	3	24, 24, 32
2	1998-10-29	11.43	166.97	1	36
3	1998-10-29	11.41	166.97	1	16
4	1998-10-29	11.45	167.04	1	24
5	1998-10-30	11.44	167.03	1	20
6	1998-10-30	11.45	167.01	1	20
7	1998-10-30	11.45	167.00	1	40
8	1998-10-30	11.44	167.00	1	16
9	1998-10-30	11.40	167.01	1	16
10	1998-10-30	11.39	166.98	1	20
11	1998-10-31	11.17	166.88	1	20
12	1998-10-31	11.17	166.86	1	24
13	1998-10-31	11.17	166.84	1	16
15	1998-11-01	11.21	166.86	1	16
16	1998-11-01	11.25	166.86	1	16
17	1998-11-01	11.28	166.86	1	16
18	1998-11-01	11.32	166.87	1	8
19	1998-11-02	11.47	166.85	1	50
20	1998-11-02	11.45	166.86	1	40
21	1998-11-02	11.44	166.79	1	28
22	1998-11-02	11.44	166.69	1	12
23	1998-11-02	11.44	166.74	1	40

Table 6: Information about the sediment samples collected in the Rongelap Atoll

Chemical preparation

The samples were prepared as sets of 24: 20 unknowns, two blanks and two IAEA standard sediment samples. Regular reagents were used, and the samples were prepared in an ordinary laboratory. The chemical preparation of the samples takes us from milled sediment to prepared AMS cathode and can be divided into six steps.

Weighing

About 2.5 g of each sediment sample (including the IAEA-367 standard sediment samples) was weighed in a 150 ml glass beaker. Two beakers were marked as “blanks”. After at least 2 hours in the oven at 100 °C the beakers were weighed again.



Figure 9: The core sampler used



Figure 10: Dr. Terry Hamilton with a nice sediment core

Dry ashing

The beakers were then put in a dry-ashing oven at 450 °C over night. Foil was put on the beakers to prevent cross contamination, and holes were punched in the foil to give the fumes a way to leave the beakers. The process reduces the carbon content in the samples.

Wet ashing

Chemicals are added the in the following order to the samples to get rid of remaining carbon. It is also first in this step the ^{242}Pu tracer is added.

- 2 ml H_2O – this prevents a heavy reaction when the acid (see below) is added to the sediments
- 1 g ^{242}Pu -tracer (127 Bq g^{-1})
- 20 ml 16M HNO_3
- 5 ml 10M HCl
- About 1.6 ml of H_2O_2 dropwise – Now watch glasses was put on the beakers and the beakers were heated at medium temperature for about 1.5 hours. Then

the watch glasses were removed and the temperature was raised so that the volumes were reduced to about 20 ml after another 30 min of heating.

- 3 · 0.8 ml of H₂O₂ dropwise during heating.

The samples were then put over to clean C-tubes together with 20 ml H₂O. The samples were now in an 8 M (approximately) nitric solution. The tubes were filled up to 50 ml with 8 M HNO₃.

Ion exchange Column procedure

Since the samples still contained some particulate matter, the 5 ml sub-samples that were to be analysed, were filtered (with a 0.45µm syringe type filter) into a new C-tube. 100 – 200 mg NaNO₂ was added to each sub-sample to transform the plutonium into +IV oxidation state, for which the ion exchange column works best, and the samples were left to de-gas (NO₂ fumes goes away). About 360 Bq ²⁴³Am tracer was also added to each sample so that the efficiency of the ion exchange column procedure could be examined. After the anion exchange columns had been generated with 20 ml 8M HNO₃, the samples were added. Here followed ordinary column extractions and elution. The column was allowed to drain in-between the washes.

- ♦ 20 ml HNO₃ – Some elements, of which Americium is of main concern, do not create anions together with NO₃⁺. The bulk of these elements therefore, unlike plutonium, do not get stuck in the anion exchanger when the HNO₃ is added, and are instead washed out.
- ♦ 20 ml HCl – Other elements, like Thorium, do create anions with NO₃⁺, but not with Cl⁺. These are washed out at this step. Plutonium does make chloride anions and are thus still stuck in the ion exchanger.
- ♦ 20 ml fresh NH₄I+HCl (1.5g NH₄I per 100 ml HCl) – Now the plutonium is eluted.

Precipitation

1.0 mg Fe in a standard iron nitrate solution (1.0 mg ml⁻¹) was added. Every sample was divided into two sub-sub-samples in two new C-tubes, because of lack of space in the C-tubes. Here we diluted to 20 ml with H₂O and added conc. NH₄OH dropwise until the yellow-brown precipitate, Iron hydroxide (FeOH(s)), started to form. The addition of H₂O is simply to mild the reaction when ammonium hydroxide (NH₄OH), a strong base, is added to the acidic sample. Then three centrifugations, each 5 minutes at about 2000 r.p.m., followed. After the fluid had been decanted off in-between the centrifugations, water were added to the C-tubes (about 10 ml) and they were mixed so that the precipitate got lose from the bottom of the tube. The second and third centrifugation was done after that the sub-sub-samples were combined to the original sub-samples again.

Cathode preparation

The iron-precipitate were dissolved in one drop of conc. HNO₃ and transferred with a Pasteur pipette to a “micro beaker” in glass (the volume of this beaker is in the order of 1 ml (≈ 15 drops)) as soon as it turned colourless. 1 or 2 drops of H₂O were used to

rinse out the C-tube. Then the micro beakers were dried under a heat lamp over night and thereafter put in an oven for oxidation. The oven was turned on and heated until it reached 800°C, when it automatically turned off. About 1 mg of high purity niobium powder was added to the sample and with a stem the samples were turned into a fine powder and the Nb-powder mixed in with the sample. With a hammer and the stem could the sample then be pressed into the cathode, a standard LLNL aluminium AMS sample holder.

Analysis

^{241}Am was measured with Ge(Li) detector systems at LLNL.

^{238}U , ^{239}Pu , ^{240}Pu , ^{241}Pu , ^{242}Pu and ^{243}Am were measured with AMS. Mass 242 was measured in a 100-ms interval together with the other isotopes of interest, which were counted in a 400-ms interval. That means that for each mass, mass 242 was counted 1/5 of the total measuring time. Each mass 2xx was measured for 10 seconds or up to a given maximum number of counts (3000), whichever came first. This 10-second measurement was repeated several times for good statistics. All uncertainties for individual results are from counting statistics, while the uncertainties in mean results are one standard deviation (1σ).

Results

Blanks and IAEA-367 standard sediment samples

The number of atoms of each isotope measured in the blanks is shown in table 7 below. Here also the mean values both for the blanks and the sediment samples are given.

ID	Date Measured	²³⁹ Pu		²⁴⁰ Pu		²⁴¹ Pu		²⁴³ Am	
		# of 10 ⁷ atoms	+/-	# of 10 ⁷ atoms	+/-	# of 10 ⁷ atoms	+/-	# of 10 ⁷ atoms	+/-
B1	2000-07-13	4.3	1.5	1.0	0.7	0.0	1.1	0.0	1.1
	2000-08-23	19.2	3.8	2.8	1.6	0.0	1.5	0.0	2.6
B2	2000-07-13	3.9	1.3	0.0	0.4	0.0	1.0	0.0	1.0
	2000-08-23	2.8	1.2	0.7	0.7	0.0	1.3	0.0	1.6
B3	2000-07-18	10.5	3.5	2.3	1.7	0.0	2.1	0.0	2.6
B4	2000-07-18	13.2	4.2	0.0	1.3	0.0	2.4	0.0	3.0
B5	2000-08-23	2.1	1.2	0.0	0.8	1.4	1.4	0.0	2.1
B6	2000-08-23	13.5	3.1	3.6	1.8	0.0	1.3	0.0	2.0
Mean blank		8.7	2.5	1.3	1.1	0.2	1.5	0.0	2.0
Mean sediment		9137	288	2106	78	30	6	0.9	2.1

Table 7: Results for the blank samples (and the mean number of atoms for the sediment samples for comparison)

ID	Date Measured	^{239,240} Pu		²⁴¹ Pu		²⁴⁰ Pu / ²³⁹ Pu	
		Bq/kg	+/-	Bq/kg	+/-	Atom ratio	+/-
Std.1	2000-07-13	45	4	136	32	30.3%	0.5%
	2000-08-23	40	1	76	31	32.1%	1.0%
	2000-08-23	41	3	267	154	31.0%	3.1%
Std.2	2000-07-13	48	3	120	28	31.9%	0.6%
	2000-08-23	38	1	121	38	29.1%	0.9%
	2000-08-23	38	1	155	49	30.6%	0.7%
Std.3	2000-07-18	43	1	95	16	28.3%	0.5%
Std.4	2000-07-18	44	1	106	24	29.6%	0.6%
Mean		42	4	134	59	30.4%	1.2%
Ref. values	2000-08-01*	38 (34.4 – 39.8)		102 (92 – 114)			

Table 8 : Results for the IAEA-367 sediment samples

* The reference values are decay corrected to 2000-08-01 (Reference date was 1990-01-01).

In table 8 above the results for the IAEA-367 standard sediment samples are given together with reference values.

Surface sediment

The activity concentrations of ^{241}Am and $^{239,240}\text{Pu}$, and the ratios ^{241}Am to $^{239,240}\text{Pu}$, ^{240}Pu to ^{239}Pu and ^{241}Pu to ^{239}Pu , are all plotted as a function of the sample location (that is as a function of latitude and longitude). The shape of the Rongelap Atoll that is made up of islands and reefs are displayed in the diagrams. The Atoll is drawn on free hand with figure 1 on page 10 in Noshkin et al. 1998, as a model. It shall by no means be seen as a detailed geographical map, but instead as a rough sketch showing the approximate shape of the atoll. In appendix III the Rongelap and the Bikini Atoll is displayed in more detail. Three sediment samples were collected at station 1, and the average value for these three samples are shown in diagrams, and used when calculating mean values of all stations etc.

In table 9 mean results and some concentration ranges are given for the 2000 data set. A more comprehensive table of all the sediment samples are included as appendix II.

	Mean results (and range)
^{241}Am [Bq/kg]	34.9 (< Det. limit – 202)
$^{239,240}\text{Pu}$ [Bq/kg]	50.3 (6.0 – 256)
$^{240}\text{Pu} / ^{239}\text{Pu}$ [atom / atom]	0.24 ± 0.03
$^{241}\text{Pu} / ^{239}\text{Pu}$ [atom / atom]	0.0035 ± 0.0013
$^{241}\text{Am} / ^{239,240}\text{Pu}$ [activity / activity]	0.70 ± 0.27

Table 9: Results for the surface sediment samples

Activity concentrations of ^{241}Am in surface sediments (0 – 4 cm) are displayed in figure 11, where also data from surveys in 1978 and 1981 are included for comparison. Only the samples north of 11° and 23 minutes N and west of 166° and 52 minutes E are included from the large 1981 sample data collection. It should be noted that the samples collected during the 1978 survey are taken at shallow depths (1 – 2 m) close to islands while the two other series are taken at larger depths and further away from islands.

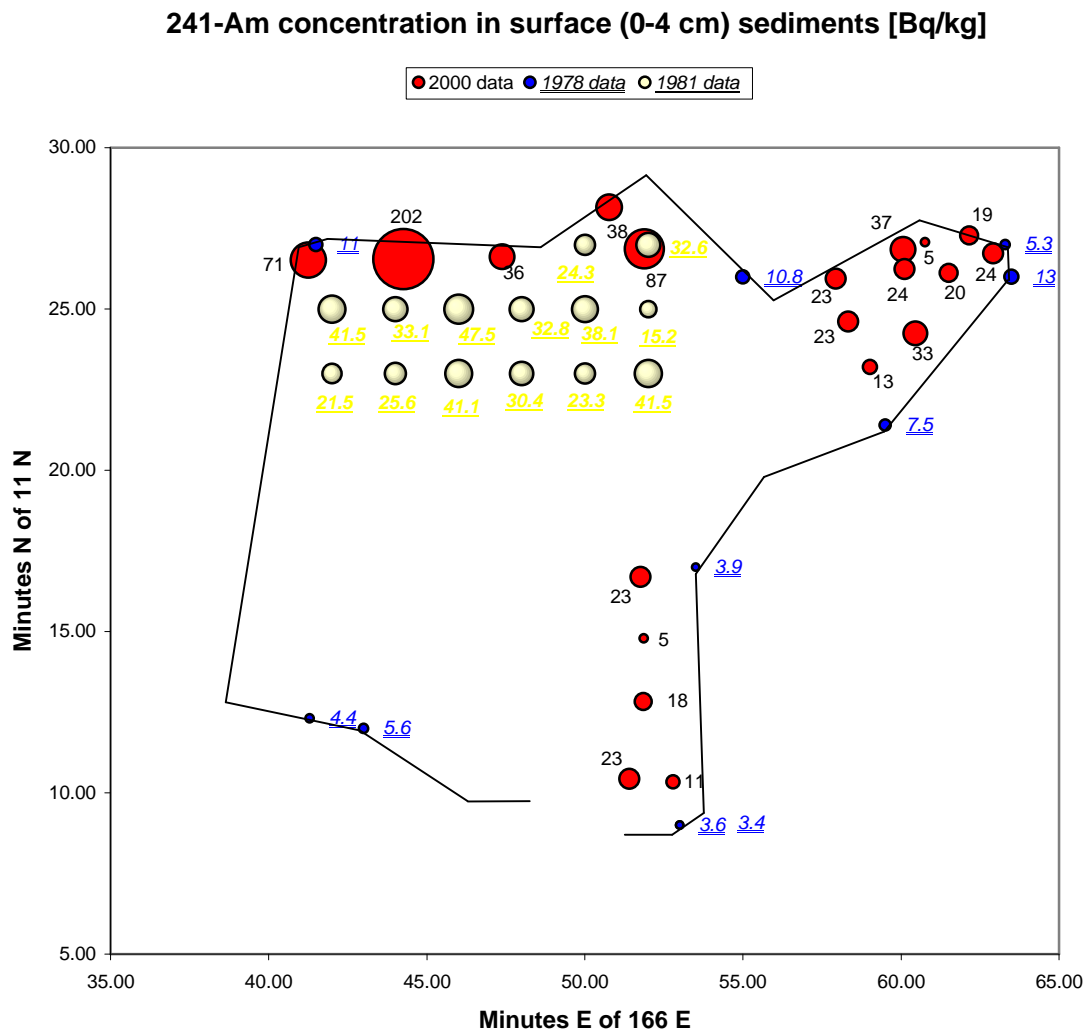


Figure 11: ^{241}Am concentrations ion surface (0-4 cm) sediments samples

The surface sediment data for $^{239,240}\text{Pu}$ are displayed in figure 12 in the same way as for ^{241}Am , with the exception that no data are available from the 1981 survey since plutonium was not analysed for these samples.

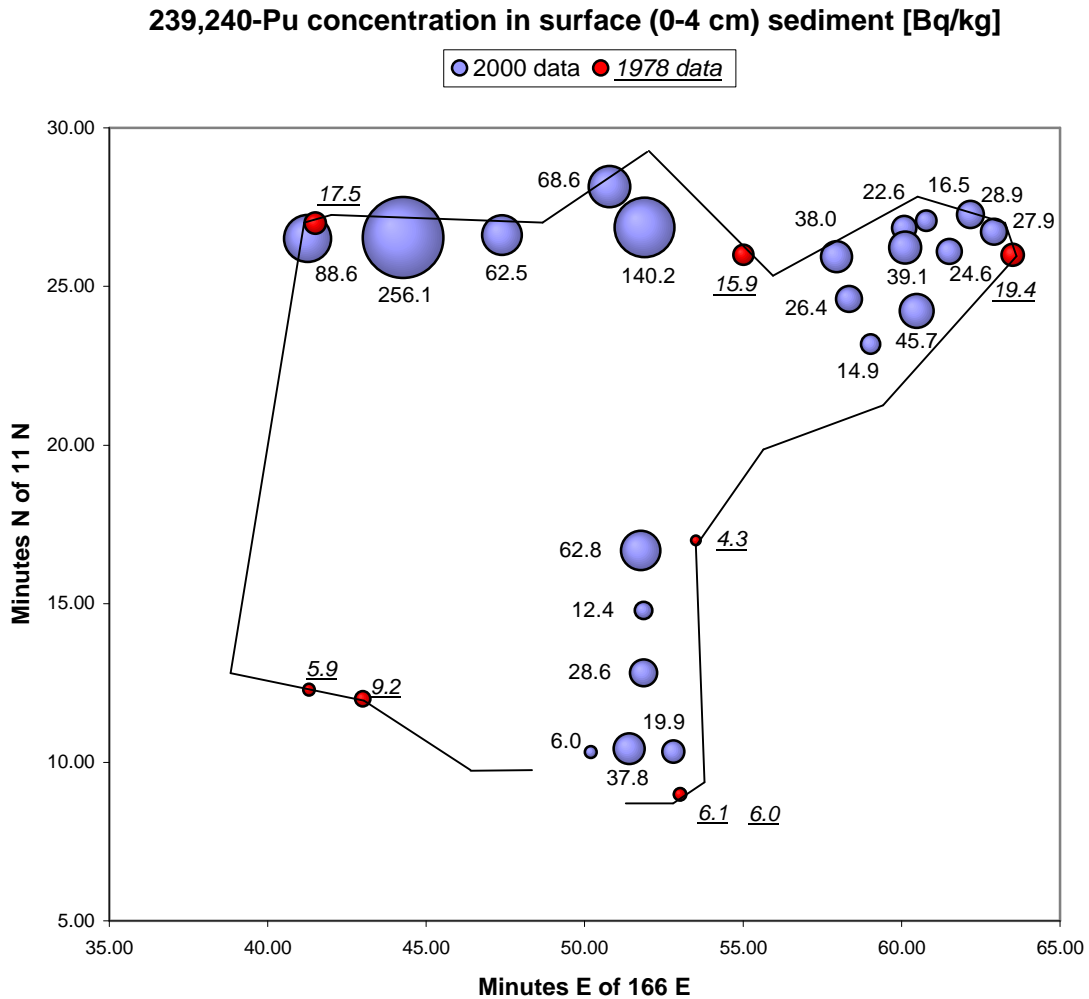


Figure 12: The $^{239,240}\text{Pu}$ concentration in surface (0-4 cm) sediment samples

Ratios for the atom abundance of ^{240}Pu and ^{241}Pu to that of ^{239}Pu in the surface sediments are shown in figures 13 and 14, respective. The activity ratio of ^{241}Am to $^{239,240}\text{Pu}$ in the surface samples is plotted in figure 15.

240/239-Pu atom ratios in surface (0-4 cm) sediment

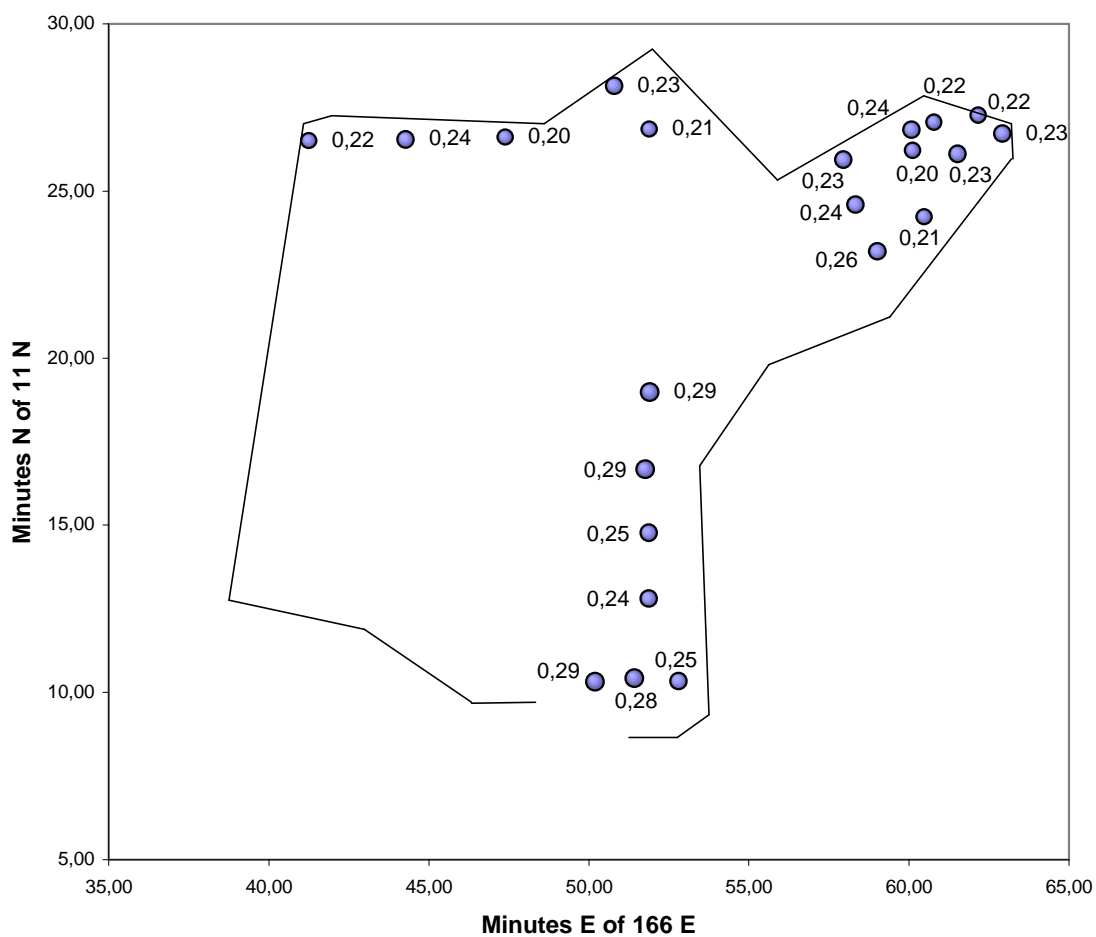


Figure 13: $^{240}\text{Pu}/^{239}\text{Pu}$ atom ratios for the surface (0-4 cm) sediment samples

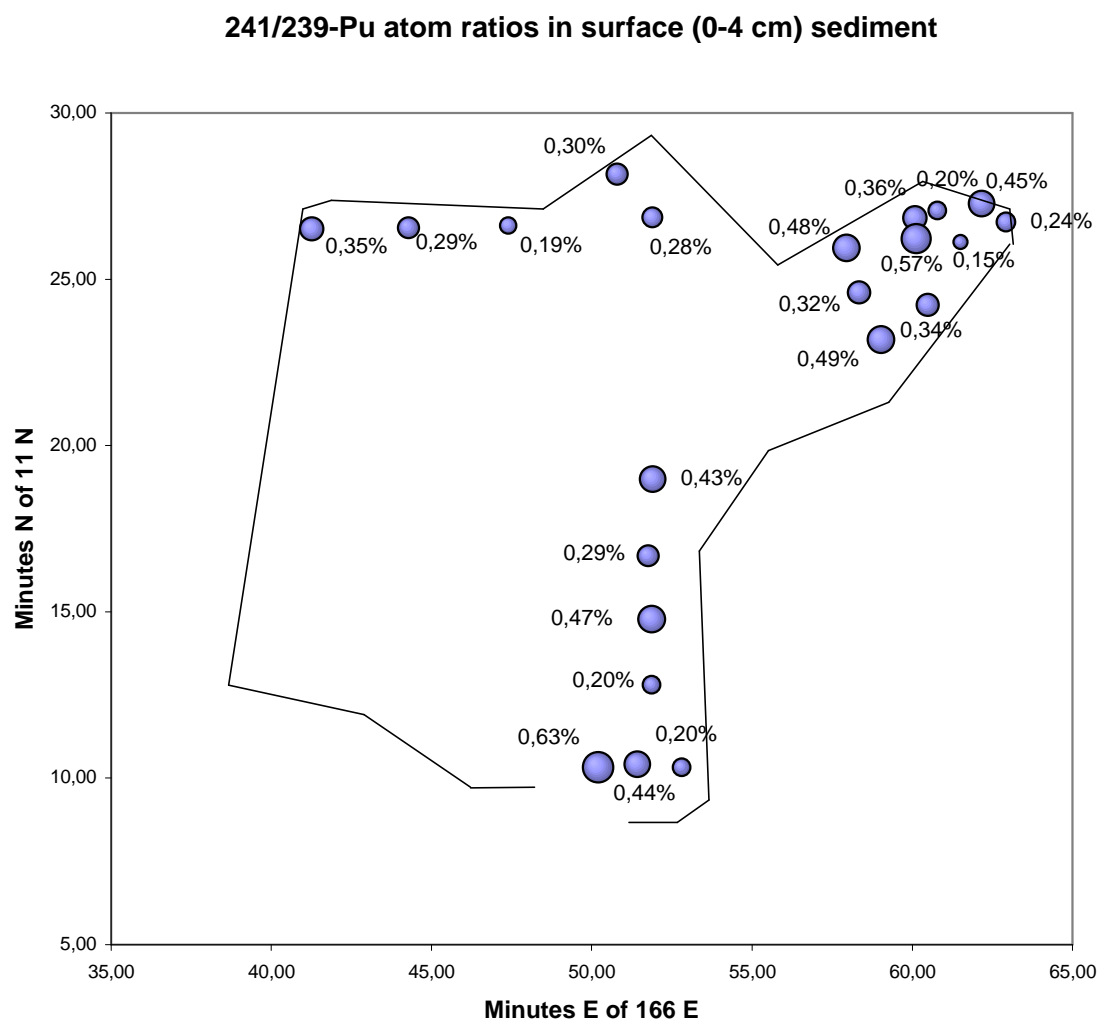


Figure 14: $^{241}\text{Pu}/^{239}\text{Pu}$ atom ratios for the surface (0-4 cm) sediment samples

241-Am / 239,240-Pu activity ratios in surface (0-4 cm) sediment

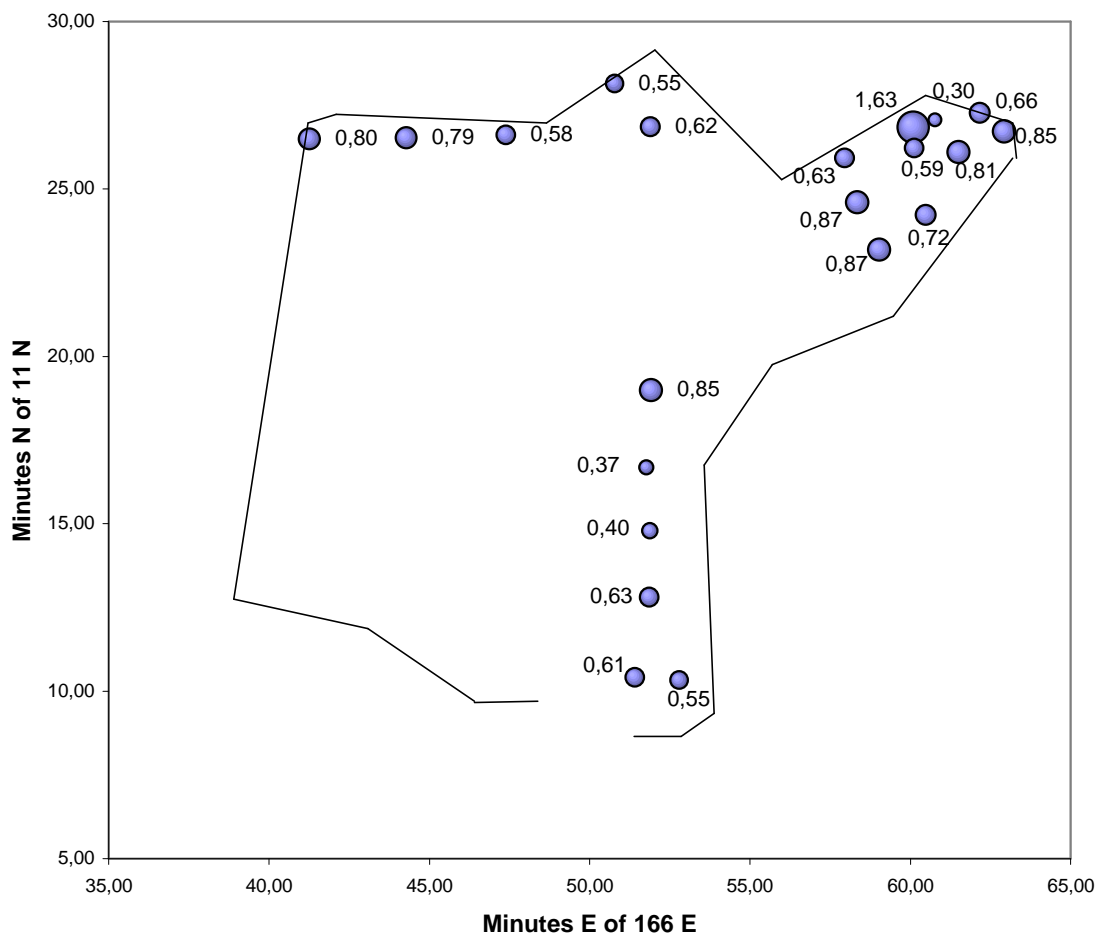


Figure 15: $^{241}\text{Am}/^{239,240}\text{Pu}$ activity ratios for the surface (0-4 cm) sediment samples

Sediment cores

All the sediment samples were collected as cores, and not as surface grabs, but only cores from five stations was analysed by me, because of time limits. The picking of which cores to analyse was based on geographical basis, as well as on the core depths. Deep cores and a large geographical spread were wanted. The location of the five sample stations chosen for core analysis is shown in figure 8. Results for the five sediment cores are displayed as a function of depth. In figure 16 and 17, the activity concentration for $^{239,240}\text{Pu}$ is plotted as a function of depth for sample stations 2, 11 and 12, and for station 19 and 23, respective.

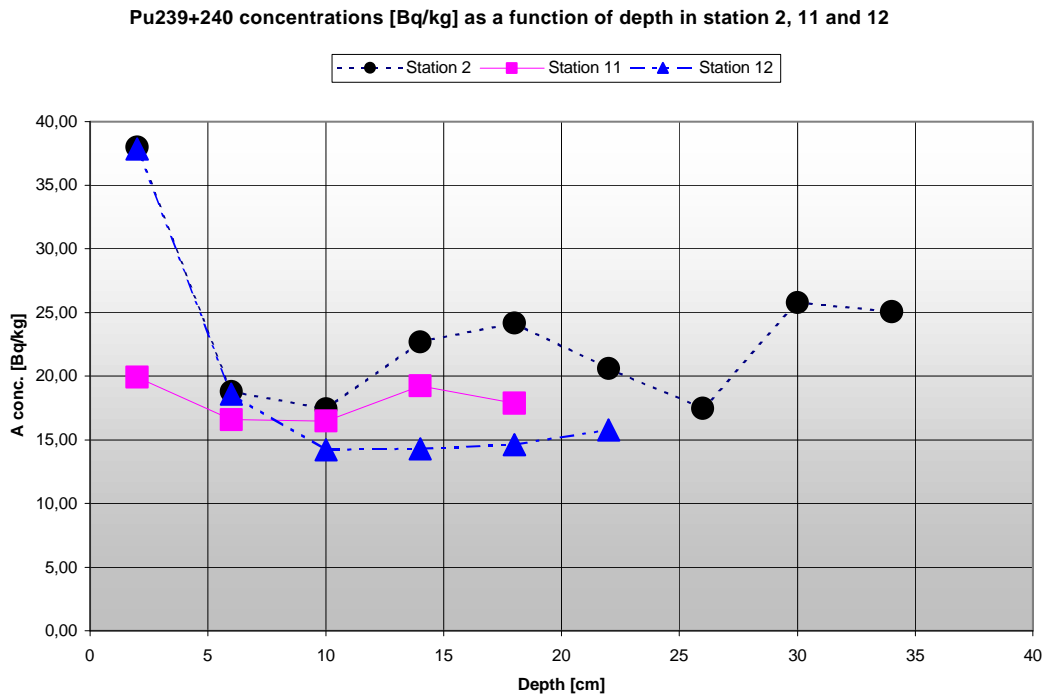


Figure 16: Vertical distribution of $^{239,240}\text{Pu}$ in sediment cores taken at stations 2, 11 and 12

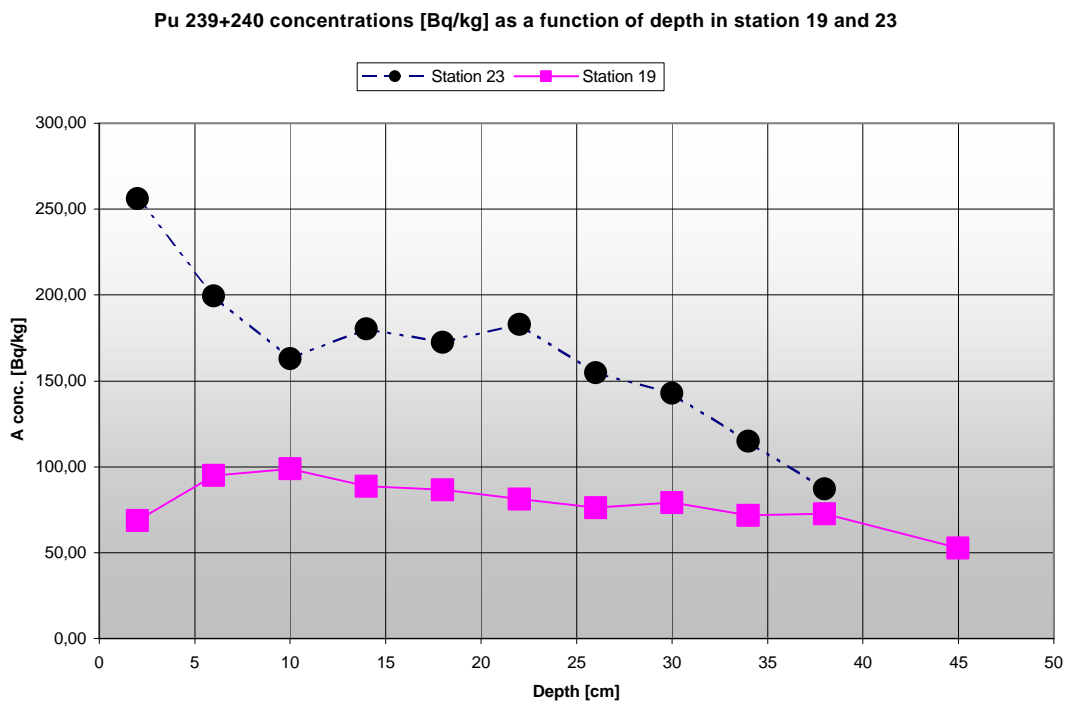


Figure 17: Vertical distribution of $^{239,240}\text{Pu}$ in sediment cores taken at stations 19 and 23

To show how the plutonium concentration varies with depth in all the cores, I have normalised to 1 for the maximum $^{239,240}\text{Pu}$ -concentration value in each core and plotted the relative concentration for the five cores as a function of depth in figure 18.

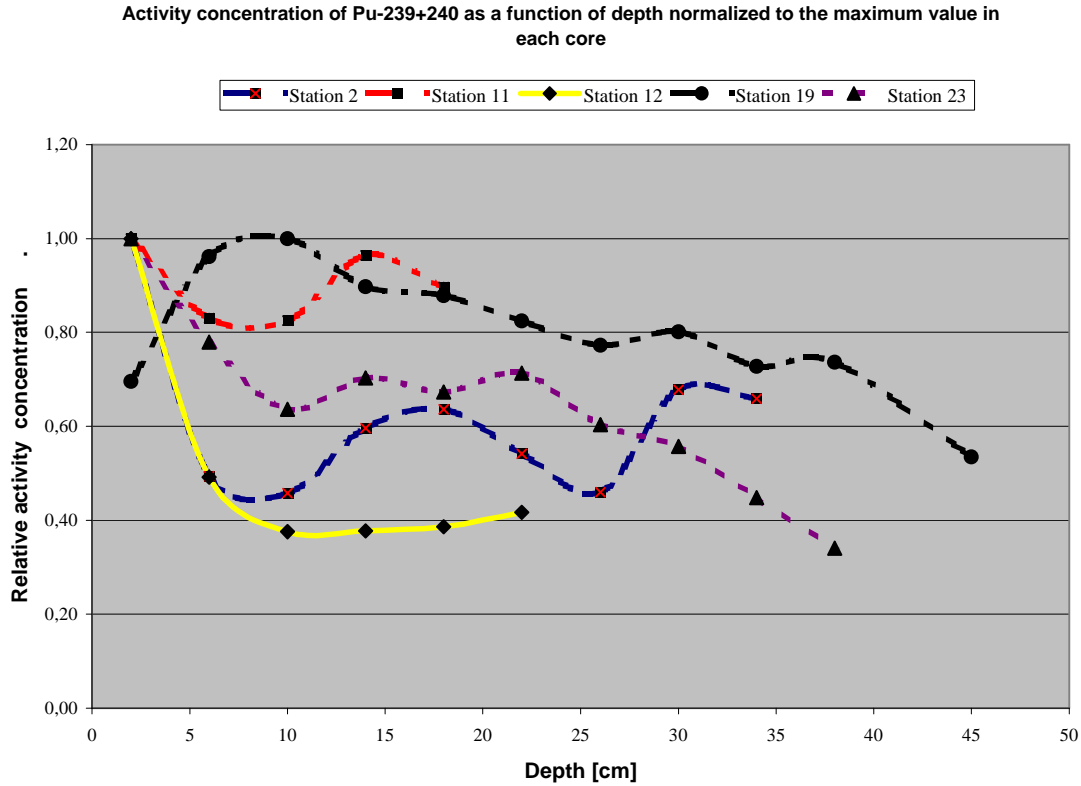


Figure 18: Activity concentration of $^{239,240}\text{Pu}$ as a function of depth normalized to the maximum value in each core

The mean activity ratio $^{241}\text{Am}/^{239,240}\text{Pu}$, and the mean atom ratios $^{240}\text{Pu}/^{239}\text{Pu}$ and $^{241}\text{Pu}/^{239}\text{Pu}$, for the five cores, are displayed in figure 19, 20 and 21, respective. The two atom ratios are shown together with the ratios for stratospheric fallout in the Northern Hemisphere and the ratios for Bravo fallout according to table 3.

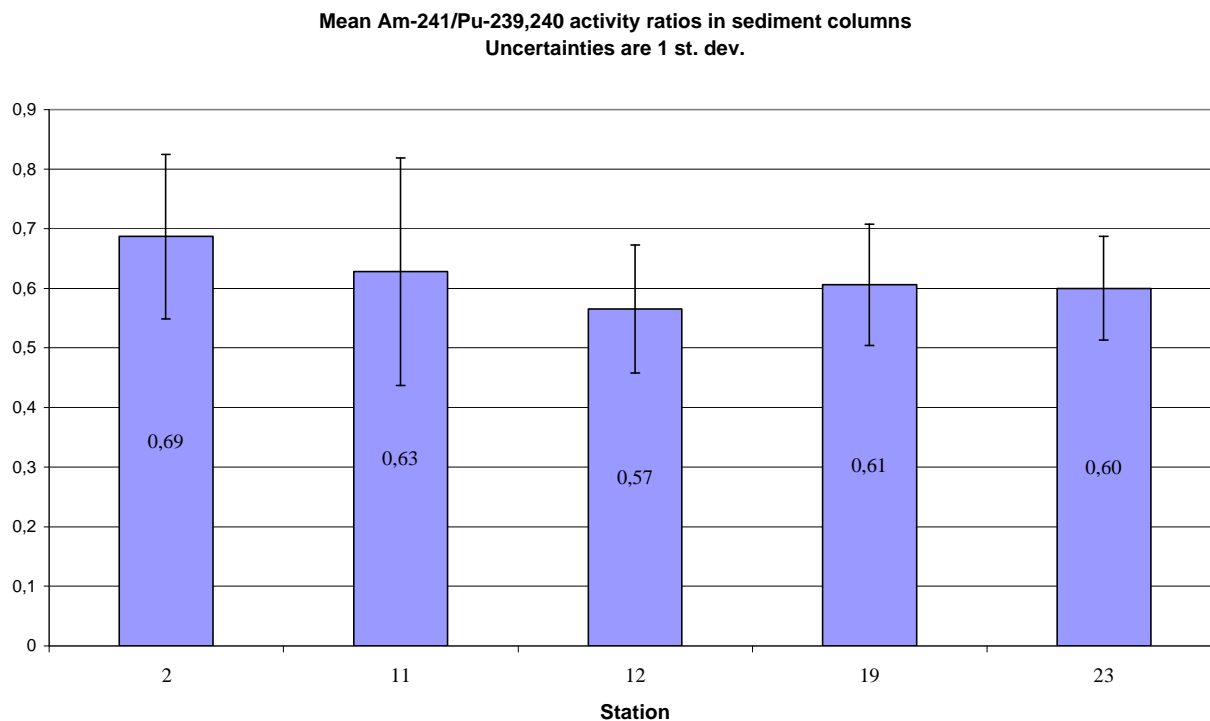


Figure 19: Mean $^{241}\text{Am}/^{239,240}\text{Pu}$ activity ratios in sediment columns

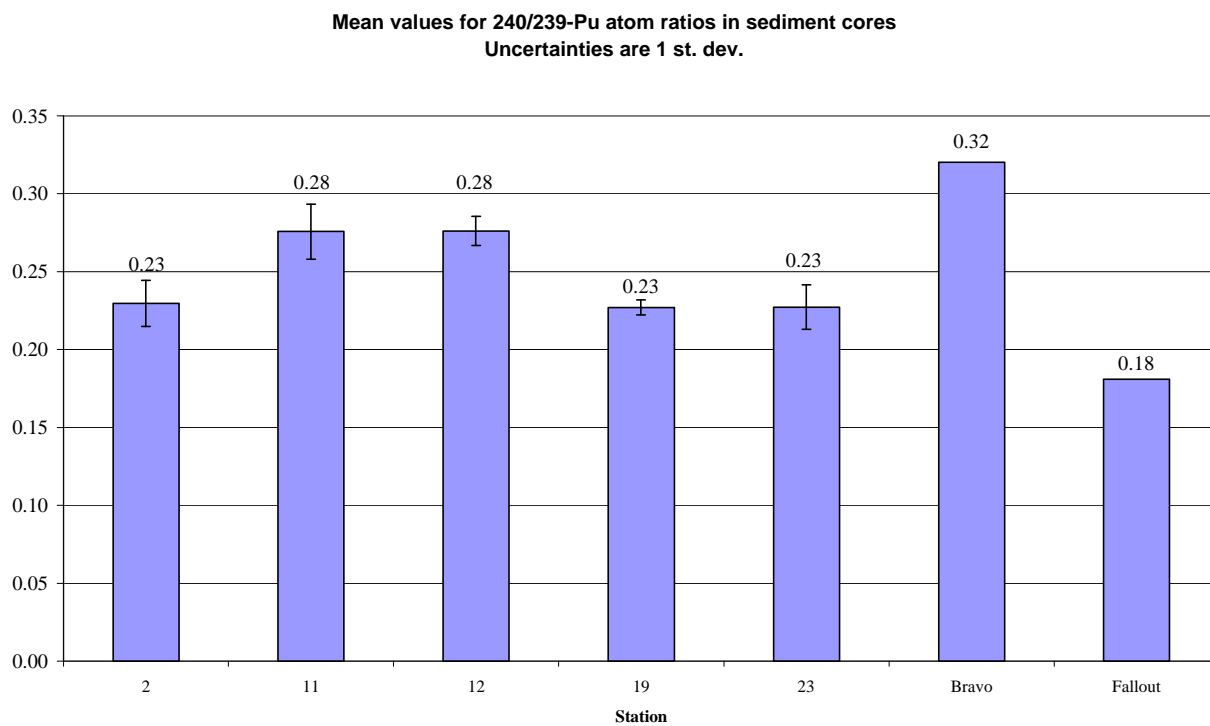


Figure 20 : Mean $^{240}\text{Pu}/^{239}\text{Pu}$ atom ratios in sediment cores

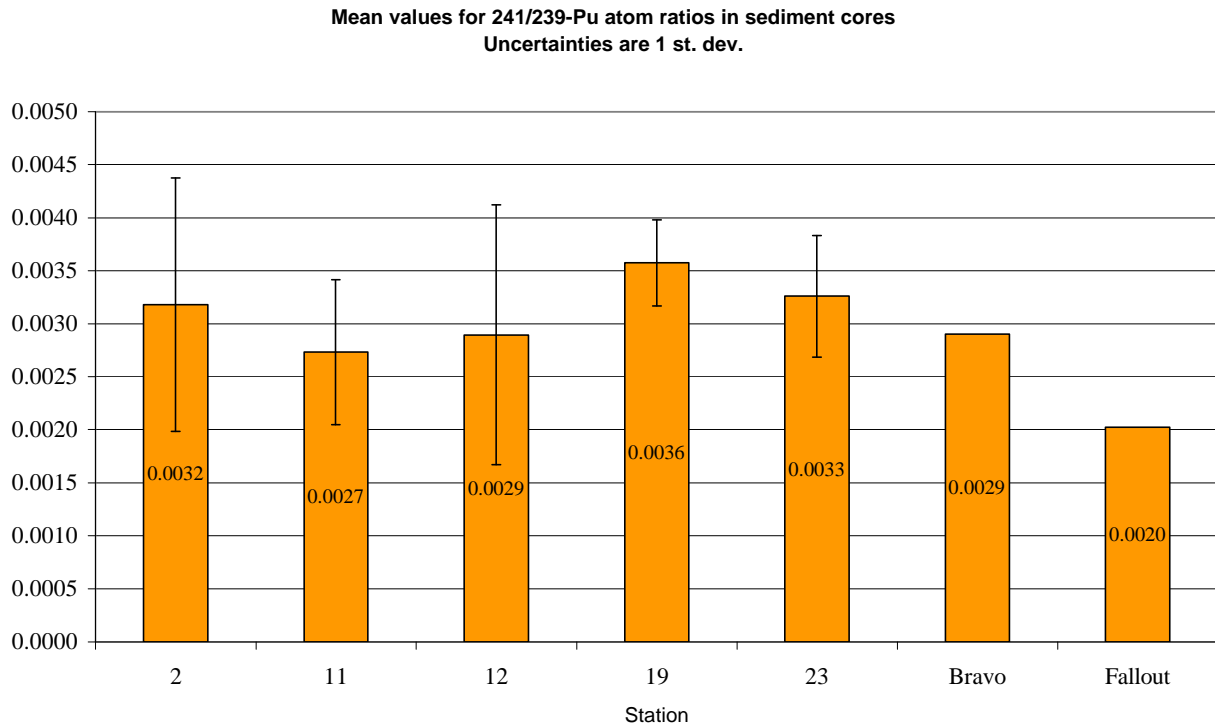


Figure 21: Mean $^{241}\text{Pu}/^{239}\text{Pu}$ atom ratios in sediment cores

Discussion

The blanks are about three orders of magnitude lower than the sediment samples for ^{239}Pu and ^{240}Pu , and about two orders of magnitude lower for ^{241}Pu . The background levels can therefore be ignored.

The measured $^{239,240}\text{Pu}$ - and ^{241}Pu - concentrations are somewhat higher than the listed values for the reference, and the values are spread over a large range.

The distribution pattern of plutonium and americium is as predicted, with highest concentrations in the Northwest corner of the atoll. Compared to the 1981 series the ^{241}Am activity concentrations in the surface sediments in the northwest (north of 11° and 23 minutes N and west of 166° and 52 minutes E) are more spread in the 2000 data set. The ^{241}Am and $^{239,240}\text{Pu}$ activity concentrations in the surface sediment samples are generally somewhat higher than the values from the 1978 series. However, as the 1978 series is collected on shallow water (1 – 2 m deep) close to islands, which is not the case for the two other series, a direct comparison cannot be made between the series.

Both ^{241}Am and $^{239,240}\text{Pu}$ have a vertical distribution that differs from that of Bikini and Enewetak Atolls (Robison et al., 1997). In four out of the five cores the Pu-concentration

was highest near the surface and decreased with depth to between 5 and 10 cm. Here concentrations were 40 – 80 % of its surface value. The concentration then changes slowly, if at all, down to the maximum core depth (20 – 50 cm). This tells us that when calculating the inventory to depths exceeding 4 cm in the Rongelap sediment, one makes an underestimation if distribution pattern for Bikini and Enewetak (Robison and Noshkin, 1998) is used. As mentioned, the reason for the relatively high concentration of Pu at larger depths in the sediment from Rongelap could be because of the presence of a more active biological environment in the sediment here.

A slight geographical variation is seen in the $^{240}\text{Pu}/^{239}\text{Pu}$ ratio both for the surface samples and the cores. The mean ratio and the range in the seven surface samples collected south of 20 minutes north of 11°N are 0.27 (0.24 – 0.29), while the mean ratio and the range in the 15 surface samples collected north of this latitude is 0.23 (0.20 – 0.26). If we make the same geographical dividing for the cores, we find that the ratios for the stations north of 20 minutes north of 11°N , station 2, 19 and 23 are 0.23 ± 0.01 , 0.23 ± 0.00 and 0.23 ± 0.01 respective. Mean ratios for the two stations south of 20 minutes north of 11°N , station 11 and 12 are 0.28 ± 0.02 and 0.28 ± 0.01 respective. This variation seems to be relevant, as both the columns and the surface samples show this result. I can however not explain the reason for this ratio-difference. One would perhaps if anything, expect a higher $^{240}\text{Pu} / ^{239}\text{Pu}$ atom ratio in the north west corner of Rongelap, where the Bravo plume crossed, than in the south. This since the Bravo $^{240}\text{Pu} / ^{239}\text{Pu}$ atom ratio is 0.32 ± 0.03 and the ratio for global stratospheric fall-out in the Northern Hemisphere, given in table 3, is 0.181 ± 0.006 . The overall mean value, 0.24 ± 0.03 , is lower than expected (0.32 ± 0.03 for Bravo fallout from table 3).

The other ratios, $^{241}\text{Pu}/^{239}\text{Pu}$ and $^{241}\text{Am}/^{239,240}\text{Pu}$ does not show any clear geographical variation, neither for surface samples nor for core samples. The estimated decay corrected (to 2000) $^{241}\text{Am}/^{239,240}\text{Pu}$ activity ratio from 1978, 0.72 ± 0.12 , is in good agreement with the measured mean result, 0.70 ± 0.29 . The larger uncertainty in the mean measured values is largely due to one value (1.63), and if this is discarded we get a mean value of 0.68 ± 0.18 . When looking at figure 19, one could perhaps think that the ratio is higher at the surface than deeper down in the sediment column, as the mean ratios for all the cores are lower than the mean surface ratio. This can however not be proven, as three of the five cores have a surface ratio that is lower than the mean ratio for that core. It seems to be just coincidence and a large fluctuation of the ratio that gives this misleading picture.

There is a large spread in the $^{241}\text{Pu}/^{239}\text{Pu}$ -atom ratio, both for the cores and the surface samples. The mean value for the surface samples, 0.0035 ± 0.0013 is somewhat higher than the decay corrected value from table 3, 0.0029 ± 0.0002 , while the mean ratios for the cores are more spread around this listed value (see figure 21).

PART 2: Measurement of Plutonium in seawater from the Marshall Islands using AMS

Background

The NE trade wind moves the lagoon surface water from the east to the west side of the lagoons in the Marshall Islands. To replace the surface water moving westward, water up-wells in the east. This way a circulation of the lagoon water is created which in turn enhances the replacement of lagoon water with surface water from the North Equatorial Pacific Ocean. The flushing time varies from one lagoon to the other, and depends among other things on the volume of the lagoon. The average depths of the lagoons are about 60 meters and the flushing-half-time for the Bikini Atoll is about a month. 99 % of the lagoon water will thereby be replaced with water from the Pacific Ocean in about 7 months (Donaldson et al., 1997). Hence, if no radionuclides were released from the sediment or from the land to the lagoon water, activity levels in the same order as for the Pacific Ocean would be found in the water. This is however not the case, and activities much higher than in the Pacific Ocean are found in both the Bikini and the Enewetak lagoon. Measurements of radionuclides in surface ocean water sampled close to and far away from the influenced atolls also indicate that this remobilisation is present. It has been found, for plutonium, that the activity concentration in the lagoon water is in relation to the activity concentration in the sediment. This implies that a steady release of radionuclides from the sediment to the lagoon water is present. Average concentrations of $^{239+240}\text{Pu}$ in lagoon water and ocean water from The Marhsall Islands are presented in table 5.

The purpose is to find out how to do AMS – measurements of plutonium from small volumes of seawater (more precise, it is lagoon water from the Bikini Atoll and open ocean water from in-between the Bikini and the Rongelap Atoll). The chemical preparation, and especially the precipitation procedure, is of main interest.

Method

Sampling

As regarding the sediment samples, I was not present at the survey when the water samples were collected. They were all collected on a depth of about 1 metre and filtered through a 0.2 μm filter. Figure 22 shows all the sample locations (sediment collecting stations as well), and the two atolls Bikini and Rongelap, are schematically marked. Table 10 gives information about the water samples and the stations.

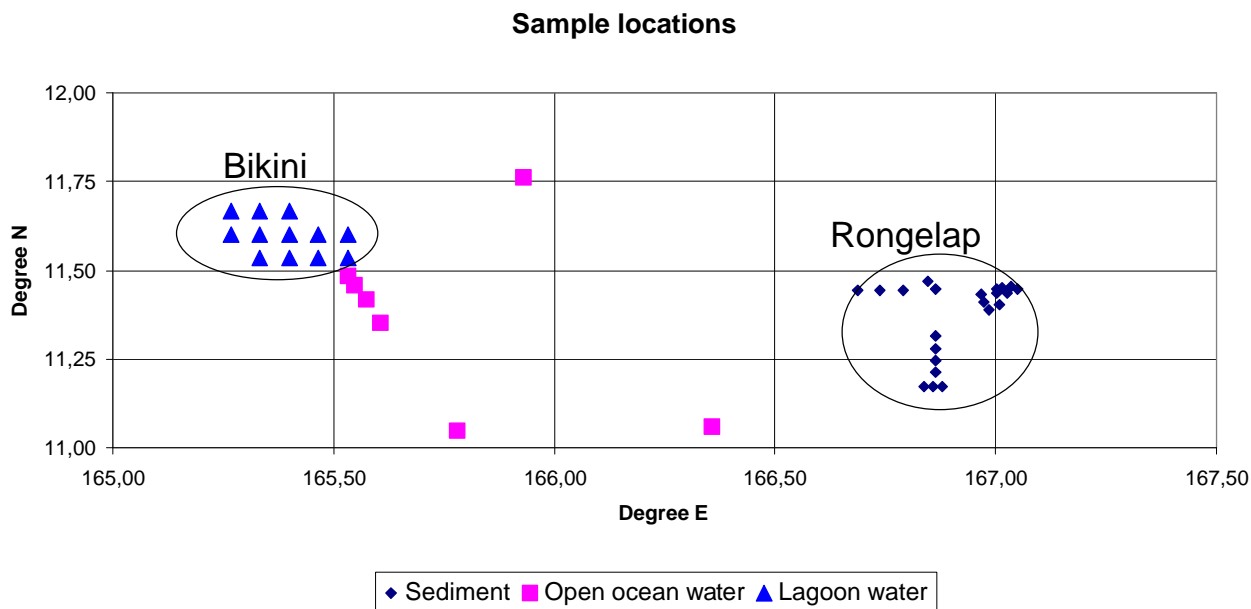


Figure 22: Sample locations

Station no.	Sampling date	Type	Degree North	Degree East	Km off Bikini	Sample volume
W1	2000-04-14	open water	11,1	166,4	161	7.6 litres
W2	2000-04-14	open water	11,8	165,9	80	7.6 litres
W3	2000-04-14	open water	11,0	165,8	48	7.6 litres
W4	2000-04-14	open water	11,4	165,6	26	7.6 litres
W5	2000-04-15	open water	11,4	165,6	9,7	7.6 litres
W6	2000-04-15	open water	11,5	165,5	4,8	7.6 litres
W7	2000-04-15	open water	11,5	165,5	1,6	7.6 litres
W8	2000-05-01	lagoon water	11,6	165,5		2 litres
W9	2000-05-01	lagoon water	11,5	165,5		2 litres
W10	2000-05-05	lagoon water	11,5	165,5		2 litres
W11	2000-05-05	lagoon water	11,5	165,4		2 litres
W12	2000-05-05	lagoon water	11,5	165,3		2 litres
W13	2000-05-05	lagoon water	11,6	165,3		2 litres
W14	2000-05-05	lagoon water	11,6	165,3		2 litres
W15	2000-05-05	lagoon water	11,7	165,3		2 litres
W16	2000-05-05	lagoon water	11,7	165,3		2 litres
W17	2000-05-05	lagoon water	11,7	165,4		2 litres
W18	2000-05-05	lagoon water	11,6	165,4		2 litres
W19	2000-05-05	lagoon water	11,6	165,5		2 litres

Table 10: Information regarding the seawater samples

Chemical preparation

General

Just as regarding the sediment samples, no special reagents and equipment was used and the work was done in an ordinary laboratory. As the chemical preparation is identical to that of the sediment preparation from the ion exchange and on, only the procedures before the ion exchange will be described here. Apart from the weighing, when about 40 g and 1000 g of each sample was put in 50 ml C-tubes respective 2 litre plastic bottles, and weighed on a digital scalar, the pre-ion exchange work principally consisted of precipitation. As the precipitation procedures is the most crucial step in the chemical preparation of these samples, and since a number of tests were conducted to find out the best way to take care of the precipitate, this part will be covered above all.

Fluride precipitation

At a fluoride precipitation of sea water the rare earth elements (REE), Ca and Mg will form fluoride complexes where Pu, Am, Th, Cm etc. will be co-precipitated. The actinides themselves also form fluoride complexes, but since the mass of this precipitate is so low, the Ca, Mg and the rare earth elements (REE) are needed to get an actual physical solid substance. Seawater contains about 400 mg l^{-1} Ca and 1270 mg l^{-1} Mg. Using 40 ml seawater we should get about 16 mg Ca and 51 mg Mg. CaF_2 and MgF_2 have the solubility $0.0016\text{g}/100 \text{ ml}$ and $0.0076\text{g}/100 \text{ ml}$ respectively, in cold water. Therefore the total weight of the CaF_2 -, and the MgF_2 - precipitate should be about 30 mg ($A_{\text{Ca}} = 40.1$, $A_{\text{F}} = 19.0$ and soluble part $\approx 0.7 \text{ mg}$ ($45 \text{ ml} \cdot 0.0016\text{g}/100 \text{ ml}$)) and 127 mg ($A_{\text{Mg}} = 24.3$, $A_{\text{F}} = 19.0$ and soluble part $\approx 3.4 \text{ mg}$ ($45 \text{ ml} \cdot 0.0076\text{g}/100 \text{ ml}$)), respectively. That means that in 45 ml water (and HF) we will have about 160 mg solid precipitate.

An advantage for this type of precipitation, when you are interested in the Pu-isotopes, is that the heavy U^{6+}O_2 - carbonate complex, does not get co-precipitated. Compared to the Pu-concentration, the U-concentration is large, and some of the uranium will be present in the complex matrixes, and hence still be present after the precipitation. Therefore, by doing a second precipitation, a better U-reduction can be achieved. Among the REE only Nd is a potential source of interference for Pu – AMS measurements. The first column washout, with 20ml 8M HNO_3 , will remove $^{3+,4+}\text{REE}$ and $^{3+,4+}\text{Am}$. Since Nd naturally is in a 3+ state, a large fraction of the present Nd will be removed.

Tests

To find out how to do the precipitation and how to continue with the precipitate in the best possible way, a number of tests were run. Since the HF precipitation of seawater basically is a mixture of CaF_2 and MgF_2 , can perhaps problems occur if the two compounds do not behave in the same way? A total number of 7 tests were run in 4 sets. The test samples were blank, Irish Sea water or lagoon water. The blank samples were made with CaCl_2 dissolved in tri-filtered H_2O at a calcium concentration similar to that of seawater. For the 100g tests 400 ml plastic beakers were used while for the smaller, 40g

tests, plastic 50 ml C-tubes were used. 16M HNO_3 was used to acidify the samples to 1M. In the first set (test 1 & 2), about 10 ml conc. (48%) HF was added dropwise to the samples of 100 g, while stirring took place on a stirring-hotplate. After one night in a refrigerator, the test samples were filtered in a vacuum system and the precipitate was collected on a 0.45 μm filter. The filters were dried for 4 hours under a heat-lamp. After not succeeding to dissolve the precipitate in 5 ml 16M HNO_3 and 500 mg boric acid in 30 ml plastic vials, they were evaporated down to dryness. 10 ml 8M HNO_3 and 10 ml $\text{Al}(\text{NO}_3)_3$ was added and the solutions were heated, as it could be that the precipitate was not soluble in cold concentrated nitric acid. The precipitate now dissolved, but as the solution cooled off precipitation took place again. The vacuum filter system used for test 1 & 2 was made of glass; a not so good material to work with together with HF, as it etches glass. In test 3 another kind of filter system, a plastic vacuum system, was used. The size of the filter was 0.8 μm , which as it turned out, was not fine enough since some of the precipitate came through the filter while some got caught. By reducing the sample volume from 100 g (≈ 100 ml) to 40 g (≈ 40 ml) in test 4 & 5, the possibility to use ordinary plastic C-tubes was given. The advantage with this was that these tubes could be used in the centrifuge and that the precipitate thus could be collected and dissolved directly in the tube after centrifugation. The filtering-step is therefore reduced. To find the recovery of the process, 54 Bq ^{242}Pu –tracer was added to each sample. Because the precipitation was rather slow in previous tests, a Ca – seed solution (4 mg Ca ml^{-1}) was used to initiate the process. After having added the HF (5 ml at test 4 & 5), 0.5 ml of this seed solution was added. Thereafter, the C-tubes were centrifuged for 5 min at about 2000 rpm. The samples were decanted off, and to the precipitate was added 5 ml 16M HNO_3 , 500 mg boric acid, 5 ml $\text{Al}(\text{NO}_3)_3$ and 7 ml H_2O . This mixture did not however manage to dissolve the precipitate. According to my supervisor, Dr. Terry Hamilton, could the reason for this be a too high concentration of salts in the solution. In test 6 & 7 the procedure was basically the same as for test 4 & 5. 7 ml HF and 1 ml seed solution was used since the precipitation process still was slow at test 4 & 5. This extra addition did not however seem to speed-up the process – it looked like the precipitation needed about 15 minutes to get started. The precipitate was dissolved in 2 ml 16M HNO_3 + 20 ml water saturated with boric acid. This time the dissolving succeeds. An Iron precipitation with 10 mg Iron (in nitric solution) followed. The iron was precipitated out with the addition of about 3 ml conc. NH_4OH . After centrifuging for 5 min at about 2000 rpm and decanting off the liquid, the iron precipitate was dissolved in 5 ml 8M HNO_3 . Hereafter followed ordinary column work and then plating for alpha spectrometry measurements of the two tests. The recovery was about 75% for the method.

Test no.	Type	Weight [g]	HF added [ml]	Filter size [mm]	Seed solution added [ml]
1	Blank	100	10	0.45	0
2	Irish				
3	Lagoon	100	10	0.8	0
4	Blank	40	5	--	0.5
5	Lagoon				
6	Blank	40	7	--	1
7	Lagoon				

Table 11: Information about Test samples no. 1 to 7

Test no.	Precipitate Dissolved in:
1	5 ml 16M HNO ₃ + 500 mg boric acid
2	
3	-----
4	5 ml 16M HNO ₃ + 500 mg boric acid + 5 ml Al(NO ₃) ₃ + 7 ml H ₂ O.
5	
6	2 ml 16M HNO ₃ + 20 ml “water saturated with boric acid”
7	

Table 12: Procedures for dissolving the test samples no. 1 to 7

The procedures used when preparing the real samples (lagoon water and open ocean water) were based on test 6 and 7. More precise “method descriptions” for the chemical preparations of these samples are included as appendix I.

Analysis

The AMS analysis was identical to that described for the sediment samples, with the exception that ²⁴³Am was not measured. Uncertainties were estimated as described under “analysis” for the sediment samples.

Results

No results were received for the open ocean water samples due to low recovery (see discussion below). The results for the lagoon water samples are given in figure 23 and table 13 below. The data for the 40 ml Irish Sea water standard samples and the 40 ml blanks is given in table 14 and 15, respective.

Station	Activity concentration [mBq/kg] blank corrected		Atom ratio	
	²³⁹⁺²⁴⁰ Pu	+/-	²⁴⁰ Pu / ²³⁹ Pu	+/-
W8	124	148	0	0.29
W9	49	104	0	0.54
W10	74	75	0.22	0.48
W11	74	90	0.62	1.33
	56	62	0.13	0.41
W12	903	153	0.10	0.05
W13	2804	711	0.28	0.14
	2431	257	0.17	0.04
W14	1289	144	0.09	0.03
W15	2830	256	0.18	0.04
	2219	196	0.14	0.03
W16	883	135	0.08	0.04
W17	447	100	0.11	0.08
W18	1410	183	0.26	0.07
	1548	191	0.20	0.06
W19	1045	209	0.19	0.09
Mean	958		0.18 (W10-19)	0.09 (W10-19)

Table 13: ^{239,240}Pu activity conc. and ²⁴⁰Pu/²³⁹Pu atom ratios for the lagoon water samples.

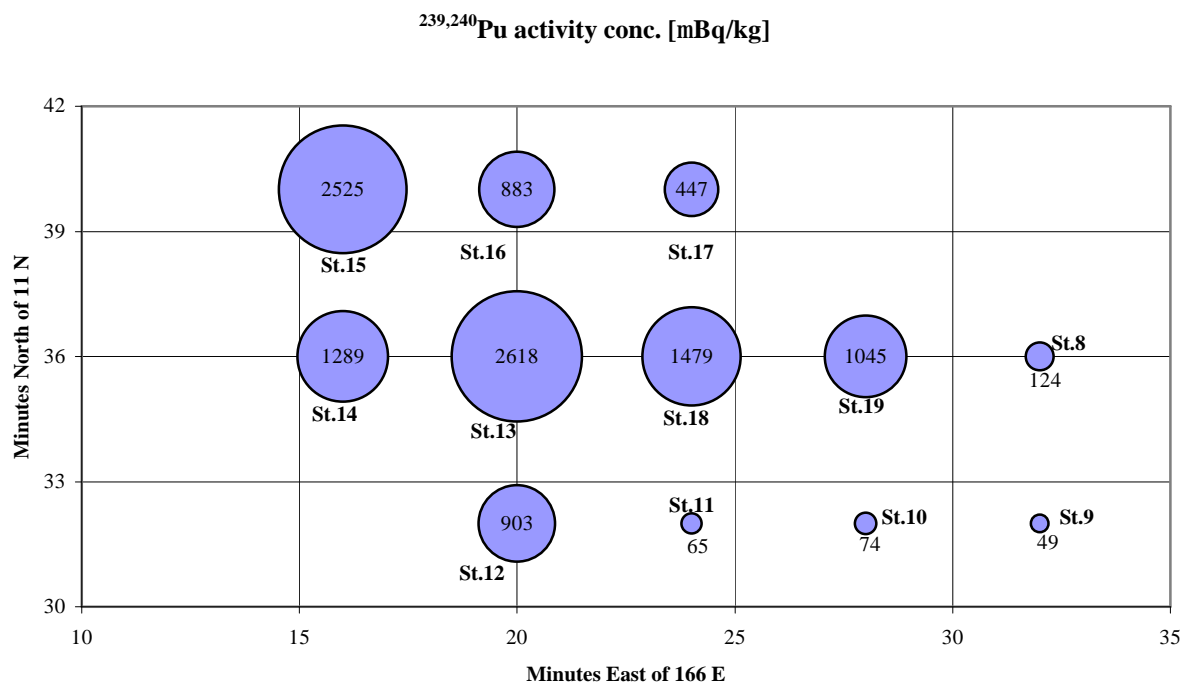


Figure23: Mean $^{239,240}\text{Pu}$ activity concentrations in lagoon water samples from the Bikini atoll

ID	Activity concentration [mBq/L] blank corrected		Atom ratio	
	$^{239+240}\text{Pu}$	+/-	$^{240}\text{Pu} / ^{239}\text{Pu}$	+/-
Std.1	16638	595	0,24	0.02
Std.2	15051	736	0,18	0.02
Std.3	17399	597	0.23	0.02
Std.4	16932	566	0.24	0.02
Mean	16505	1019	0.22	0.03
Ref. value	13200	264		

Table 14: Results for the IAEA-381 Irish Sea water samples

Number of 10^6 $^{239+240}\text{Pu}$ atoms		
	$^{239+240}\text{Pu}$	+/-
Blank 1	1.1	0.8
Blank 2	2.5	0.8
Blank 3	1.6	0.5
Blank 4	1.5	1.5
Mean	1.7	0.6
Mean for the lagoon water samples	39	31

Table 15: Results for the blank samples (and the mean number of atoms in the lagoon water samples for comparison)

Discussion

When the open ocean water samples had been centrifuged for 15 minutes and the fluid was to be decanted off, the precipitate did not stick to the bottle but was instead partly associated with the liquid phase. This way some precipitate was lost and/or some liquid was still present after the decanting. Because of this the recovery was very bad for these samples, and no results could therefore be received. The reason that we did not have this problem with the lagoon water samples could be that centrifugation was done directly after that the C-tubes was taken out of the refrigerator (e.g. no transfer to another container was made). The fact that the precipitate easily was maintained in the 2 L bottles (as it was stuck to the inside walls of the bottles), when the bulk of the liquid phase was removed immediately after that the bottles had been taken out of the refrigerator, indicates that this is the case. What would be needed as an additional step in the procedure for the open ocean water samples is to leave the precipitate to settle over night in the fridge after it has been transferred to the 250 ml bottles, and this way let it get stuck to the container walls. Another way would perhaps be to skip the transferring of the sample to a smaller container. This can be done if one from start has a bottle that can be used in the centrifuge (like for the lagoon water samples). I do however not know if centrifugation-bottles of the required size (1-2 L), and centrifuges for such, exist.

The $^{239,240}\text{Pu}$ concentrations in the standard sample were fairly consistent with the four duplicates within 13.5% from each other. Although, the mean value was about 25% higher than the reference value. As this also was the case for the soil standards, for which the activities for $^{239,240}\text{Pu}$ and ^{241}Pu was 11% and 31% higher than the reference values, respective (see table 8), this implies that the measurements generally overestimated the concentrations for the measured plutonium isotopes. The blank results show that the results for the samples W8 - W11 are very unreliable, since they are so close to the background concentrations. This is also indicated in the uncertainties for these results. Another uncertainty factor, for these samples in particular due to the location of these sampling stations (near the main passes into the lagoon), is the possibility of a rather great influence of the tide. This since there is a diluting effect from open ocean water

with lower Pu-concentration coming into the lagoon with the tide. This means that the activity concentration varies during the day, and the actual time on the day of the sample collection is crucial.

Using the data presented and discussed above (60m is the mean depth of the Marshall Islands atolls (here used as the mean depth for the Bikini Atoll); $629 \cdot 10^6 \text{ m}^2$ is the area of the Bikini Atoll; $958 \text{ } \mu\text{Bq L}^{-1}$ is the mean activity concentration for $^{239,240}\text{Pu}$ in the lagoon water of Bikini Atoll), the total $^{239,240}\text{Pu}$ -activity in the lagoon water can be estimated to be about 36 GBq. Since the $^{239,240}\text{Pu}$ -concentration in the lagoon water is well above that of the open ocean water, there must be a constant release of plutonium from the sediments. A very rough estimation of the amount of this release can be made. The $^{239,240}\text{Pu}$ activity entering the lagoon with the open ocean water can then be neglected, as the concentration is about a factor hundred lower than for the lagoon water (see table 5). The flushing half-time for the Bikini lagoon is about 1 month, and if we assume that the water that leaves the lagoon has a concentration equal to the mean value for the lagoon water, the least amount of $^{239,240}\text{Pu}$ that must be released in one month from the sediments to the water to keep the water concentration constant, is 18 GBq. It has then been assumed that all of the water that has entered the lagoon during this month, which leaves the basin, has the same activity concentration as when it entered (zero that is in this estimation). If we instead use the lagoon water concentration value listed in table 5, 1.54 Bq m^{-3} , the release would be about 60% more.

As the ratios shows such a large spread it is not easy to make any conclusion based on these data. It seems however that the ratio is closer to that of global fallout than to that of Bravo fallout.

Acknowledgement

This work was performed under the auspices of the U. S. Department of Energy by the University of California, Lawrence Livermore National Laboratory under Contract No. W-7405-Eng-48.

I would like to thank Mats Eriksson for taking time to read this thesis, and for giving me such valuable feedback.

Per Roos has also helped me and guided me in important lagoon-matters, and for that I like to thank him.

References

Cooper, L. W.; Kelley, J. M.; Bond, L. A.; Orlandini, K. A.; Grebmeier, J. M. *Sources of the transuranic elements plutonium and neptunium in arctic marine sediments*. Marine Chemistry, vol. 69, no. 3, p 253 – 276, 2000.

Cronkite, R. A.; Conrad, R. A.; Bond, V. P. *Historical events associated with fallout from Bravo shot – operation Castle and 25 Y of medical findings*. Health Physics, vol. 73, no. 1, p 176 – 186, 1997.

Donaldson, L. R.; Seymour, A. H.; Nevissi, A. H. *University of Washington's radioecological studies in the Marshall Islands, 1946-1977*, Health Physics, vol. 73, no.1, p 214 – 222, 1997.

Draganic´, I.G.; Draganic´, Z.D.; Adloff, J-P. *Radiation and Radioactivity on earth and beyond..* Boca Raton, Florida: CRC Press, Inc., p 22 – 28, 1989.

Eisenbud, M. *Monitoring distant fallout: The role of the atomic energy commission health and safety laboratory during the pacific tests, with special attention to the events following Bravo*. Health Physics, vol. 73, no. 1, p 21 – 27, 1997.

Fifield, L. K.; Gresswell, R. G.; di Tada, M. L.; Ophel, T. R.; Day, J. P.; Clacher, A. P.; King, S. J.; Priest, N. D. *Accelerator mass spectrometry of plutonium isotopes*. Nuclear Instruments and Methods in Physics Research, B 117, p 295 – 303, 1996.

Fifield, L. K. *Accelerator mass spectrometry and its applications*. Rep. Prog. Phys. 62, p 1223 – 1274, 1999.

Fifield, L. K. *Advances in accelerator mass spectrometry*. Nuclear Instruments and Methods in Physics Research, B 172, p 134 – 143, 2000.

Firestone, R. B. *Table of Isotopes - eight edition*. John Wiley & sons, Inc., 1996.

Hotchkis, M.; Fink, D.; Tuniz, C.; Vogt, S. *Accelerator mass spectrometry analyses of environmental radionuclides: sensitivity, precision and standardization*. Applied Radiation and Isotopes, 53, p 31 – 37, 2000.

IAEA, *The Radiological situation at the atolls of Mururoa and Fangataufa, Main report, Annex IV: Some fusion physics and the testing of nuclear weapons.*, Radiological assessment reports series, IAEA, p 263 – 269, 1998.

IPPNW and IEER (International Physicians for the Prevention of Nuclear War and the Institute for Energy and Environmental Research). *Plutonium: Deadly gold of the Nuclear Age*. International Physicians Press, Cambridge, Massachusetts. p 259 – 261; 294 – 304, 1992, second printing in 1995 with corrections.

Krane, K. S. *Introductory Nuclear Physics.*, John Wiley & Sons, Inc, printed in U.S.A., p 478 – 558, 1988.

McAninch, J. E.; Hamilton, T. F.; Brown, T. A.; Jokela, T. A.; Knezovich, J. P.; Ognibene, T. J.; Proctor, I. D.; Roberts, M. L.; Sideras-Haddad, E.; Southon, J. R.; Vogel, J. S. *Plutonium measurements by accelerator mass spectrometry at LLNL.* Lawrence Livermore National Laboratory, Livermore, CA, Preprint UCRL-JC-136204, 1999

McAninch, J. E.; Hamilton, T. F. *Measurement of plutonium and other actinide elements at the center for accelerator mass spectrometry: A comparative assessments of competing techniques.* Lawrence Livermore National Laboratory, Livermore, CA, UCRL – ID – 133118, 1999.

Noshkin, V. E.; Robison, W. L.; Eagle, R. J.; Wong, K. M. *Radionuclides in sediments and seawater at Rongelap Atoll.* Lawrence Livermore National Laboratory, Livermore, CA, UCRL – ID – 130250, 1998.

Noshkin, V. E.; Eagle, R. J.; Wong, K. M.; Robison, W. L. *Sediment studies at Bikini Atoll part 2. Inventories of Transuranium elements in surface sediments.* Lawrence Livermore National Laboratory, Livermore, CA, UCRL – LR – 129379, 1997a.

Noshkin, V. E.; Eagle, R. J.; Robison, W. L. *Fine and coarse components in surface sediments from Bikini lagoon.* Lawrence Livermore National Laboratory, Livermore, CA, UCRL – ID – 126358, 1997b.

Pentreath, R. J.; *The analysis of Pu in environmental samples: A brief historical perspective.* Applied Radiation and Isotopes, vol. 46, no. 11, p 1279 – 1285, 1995.

Robison, W. L.; Noshkin, V. E.; Conrado, C. L.; Eagle, R. J.; Brunk, J. L.; Jokela, T. A.; Mount, M. E.; Philips, W. A.; Stoker, A. C.; Stuart, M. L.; Wong, K. M. *The Northern Marshall Islands radiological survey: data and dose assessments.* Health Physics, vol. 73, no. 1, p 37 – 48, 1997.

Robison, W. L.; Noshkin, V. E. *Radionuclide characterization and associated dose from long-lived radionuclides in close-in fallout delivered to the marine environment at Bikini and Enewetak atolls.* Lawrence Livermore National Laboratory, Livermore, CA, UCRL-JC-130230, Preprint, 1998.

Simon, S. L. *A brief history of people and events related to atomic weapons testing in the Marshall Islands.* Health Physics, vol. 73, no. 1, p 5 – 20, 1997.

Simon, S. L.; Robison, W. L. *A compilation of the nuclear weapons test detonation data for U.S. Pacific Ocean tests.* Health Physics, vol. 73, no. 1, p 258 – 264, 1997a.

Simon, S. L.; Graham, J. C. *Findings of the first comprehensive radiological monitoring program of the republic of the Marshall Islands*. Health Physics, vol. 73, no. 1, p 66 – 85, 1997b.

Sutcliffe, W. G.; Condit, R. H.; Mansfield, W. G.; Myers, D. S.; Layton, D. W.; Murphy, P. W. *A Perspective on the Dangers of Plutonium*. Lawrence Livermore National Laboratory, Livermore, CA, UCRL-JC-118825, 1995.

Appendix I: Fluoride precipitation on sea water samples

40 ml Lagoon water samples in 50 ml C-tubes

1. Add about 65 mg CaCl_2 to 40 ml water to make the blanks
2. Add 2 ml conc. HNO_3 and mix well
3. Add 0.322 g (0.3 ml) $19.5 \text{ Bq g}^{-1} {}^{242}\text{Pu}$ – tracer
4. Let equilibrate for 2h
5. Add 7 ml HF (48%) in 1ml increments. Mix well in between.
6. Add 1 ml seed solution (4 mg Ca ml^{-1})
7. Let stand over night in a fridge to enhance the formation of fluoride precipitate
8. Centrifuge for 5 min at about 2000 rpm.
9. Decant the liquid
10. Add 15 ml H_2O
11. Add 5 ml 16M HNO_3
12. Add 20 ml saturated Boric acid solution
13. Add 1 ml iron solution (10 mg ml^{-1}) and mix well
14. Add 5-10 ml NH_4OH dropwise until precipitation takes place
15. Centrifuge for 5 min at about 2000 rpm.
16. Decant the liquid
17. Add 5 ml 8M HNO_3
18. Add 100 – 200 mg NaNO_2 . Allow to de-gas
19. Add to prepared column and go on as before (with sediment samples)

1 Litre open ocean water samples in 2 L plastic bottles

1. Add 3.75 g CaCl_2 to the blanks
2. Add 50 ml conc. HNO_3 and mix well
3. Add 0.322 g (0.3 ml) $19.5 \text{ Bq g}^{-1} {}^{242}\text{Pu}$ – tracer
4. Let equilibrate for 2h
5. Add 150 ml 48% HF in 25-ml increments. Mix well in-between
6. Let the bottles stand in a fridge over night to enhance the formation of fluoride precipitate
7. Decant off so that the volume becomes about 200 ml
8. Pour this 200 ml in a clean 250 ml plastic centrifuge-bottle
9. Rinse the 2L-bottles with up to 50 ml H_2O to get as much of the precipitate over to the 250 ml-bottles as possible
10. Centrifuge for 15 min at about 2000 rpm.
11. Decant the liquid
12. Add 60 ml H_2O
13. Add 25 ml 16M HNO_3
14. Add 80 ml saturated boric acid solution
15. Add 2 ml iron solution (10 mg ml^{-1}) and mix well
16. Add 25-45 ml NH_4OH until precipitation takes place
17. Centrifuge for 15 min at about 2000 rpm.
18. Decant the liquid
19. Add 10 ml 8M HNO_3
20. Add 200 - 400 mg NaNO_2 . Allow to de-gas
21. Add to prepared column and go on as before (with sediment samples)

Appendix II: Results for the sediment samples

Description	Measured for Pu (year 2000)	Activity conc. [Bq/kg]				Isotope Ratios: Pu - 2xx / 239			
		Pu-239,240	+/-	Am-241	+/-	Pu-240	+/-	Pu-241	+/-
STA1 0-4cm	23-aug	26.4	0.6	17	3	0.23	0.01	0.23%	0.08%
STA1 0-4cm	23-aug	31.3	0.6	30	5	0.24	0.01	0.12%	0.06%
STA1 0-4cm	23-aug	26.1	0.6	25	7	0.22	0.01	0.35%	0.10%
STA2 0-4cm	23-aug	38.0	0.8	24	3	0.23	0.01	0.48%	0.10%
STA2 4-8cm	18-jul	18.9	0.9	16	4	0.24	0.01	0.44%	0.13%
STA2 8-12cm	18-jul	17.5	0.9	9	5	0.25	0.01	0.17%	0.09%
STA2 12-16cm	18-jul	22.8	1.0	14	4	0.22	0.01	0.31%	0.11%
STA2 16-20cm	18-jul	24.3	1.0	0		0.24	0.01	0.37%	0.12%
STA2 20-24cm	18-jul	20.7	0.9	15	2	0.24	0.01	0.42%	0.15%
STA2 24-28cm	18-jul	17.5	0.9	0		0.22	0.01	0.16%	0.08%
STA2 28-32cm	18-jul	25.9	1.1	15	4	0.21	0.01	0.30%	0.10%
STA2 32-36cm	18-jul	25.1	1.1	22	8	0.21	0.01	0.21%	0.09%
STA3 0-4cm	13-jul	26.5	1.8	23	4	0.24	0.01	0.32%	0.09%
STA4 0-4cm	23-aug	28.9	0.6	19	4	0.22	0.01	0.45%	0.12%
STA5 0-4cm	13-jul	24.7	1.6	20	4	0.23	0.01	0.15%	0.07%
STA6 0-4cm	18-jul	16.5	0.9	5	4	0.22	0.01	0.20%	0.09%
STA7 0-4cm	18-jul	22.8	1.1	37	8	0.24	0.01	0.36%	0.10%
STA8 0-4cm	18-jul	39.3	1.9	23	3	0.20	0.01	0.57%	0.10%
STA9 0-4cm	18-jul	46.0	2.0	33	4	0.21	0.01	0.34%	0.07%
STA10 0-4cm	18-jul	15.0	0.8	13	2	0.26	0.01	0.49%	0.15%
STA11 0-4cm	18-jul	20.1	1.0	11	3	0.25	0.01	0.20%	0.09%
STA11 4-8cm	23-aug	16.6	0.4	14	4	0.28	0.01	0.31%	0.14%
STA11 8-12cm	23-aug	16.4	0.4	8	6	0.27	0.01	0.36%	0.13%
STA11 12-16cm	23-aug	19.2	0.4	0		0.30	0.01	0.30%	0.11%
STA11 16-20cm	23-aug	17.9	0.5	0		0.28	0.01	0.20%	0.12%
STA12 0-4cm	18-jul	38.0	1.7	23	8	0.28	0.01	0.44%	0.09%
STA12 4-8cm	23-aug	18.6	0.5	12	5	0.28	0.01	0.28%	0.13%
STA12 8-12cm	23-aug	14.2	0.4	0		0.27	0.01	0.21%	0.11%
STA12 12-16cm	23-aug	14.3	0.4	0		0.29	0.01	0.34%	0.15%
STA12 16-20cm	23-aug	14.6	0.4	0		0.27	0.01	0.36%	0.15%
STA12 20-24cm	23-aug	15.8	0.4	7	3	0.26	0.01	0.09%	0.09%
STA13 0-4cm	18-jul	6.1	0.4	0		0.29	0.02	0.63%	0.29%
STA15 0-4cm	18-jul	28.7	1.4	18	4	0.24	0.01	0.20%	0.07%
STA16 0-4cm	18-jul	12.4	0.7	5	2	0.25	0.01	0.47%	0.18%
STA17 0-4cm	18-jul	63.2	2.4	23	8	0.29	0.01	0.29%	0.06%

Description	Measured for Pu (year 2000)	Activity conc. [Bq/kg]				Isotope Ratios: Pu - 2xx / 239			
		Pu- 239,240	+/-	Am-241	+/-	Pu-240	+/-	Pu-241	+/-
STA18 0-4cm*	18-jul	---	--	--	--	0.29	0.01	0.43%	0.10%
STA19 0-4cm	18-jul	68.9	2.7	38	5	0.23	0.01	0.30%	0.08%
STA19 4-8cm	23-aug	94.8	1.2	48	11	0.22	0.00	0.37%	0.06%
STA19 8-12cm	23-aug	98.6	1.2	56	7	0.23	0.00	0.37%	0.05%
STA19 12-16cm	23-aug	88.5	1.0	63	3	0.22	0.00	0.33%	0.05%
STA19 16-20cm	23-aug	86.6	1.1	59	3	0.23	0.00	0.34%	0.05%
STA19 20-24cm	23-aug	81.3	1.0	52	2	0.23	0.00	0.33%	0.06%
STA19 24-28cm	23-aug	76.2	1.0	36	9	0.23	0.00	0.31%	0.06%
STA19 28-32cm	23-aug	79.0	1.0	65	7	0.23	0.00	0.41%	0.07%
STA19 32-36cm	23-aug	71.7	1.0	42	4	0.23	0.00	0.40%	0.07%
STA19 36-40cm	23-aug	72.6	1.1	43	4	0.22	0.01	0.42%	0.08%
STA19 40-50cm	23-aug	52.8	0.8	28	5	0.24	0.01	0.35%	0.08%
STA20 0-4cm	18-jul	140.8	5.3	87	6	0.21	0.00	0.28%	0.04%
STA21 0-4cm	18-jul	62.8	2.5	36	3	0.20	0.01	0.19%	0.07%
STA22 0-4cm	13-jul	89.0	6.3	71	13	0.22	0.00	0.35%	0.05%
STA23 0-4cm	13-jul	257.2	17.8	202	6	0.24	0.00	0.29%	0.03%
STA23 4-8cm	18-jul	200.4	8.4	124	9	0.21	0.00	0.35%	0.05%
STA23 8-12cm	18-jul	163.7	5.4	99	6	0.25	0.00	0.43%	0.05%
STA23 12-16cm	18-jul	181.0	6.3	96	11	0.24	0.00	0.29%	0.05%
STA23 16-20cm	18-jul	173.2	5.6	89	4	0.23	0.00	0.31%	0.04%
STA23 20-24cm	18-jul	183.5	6.0	91	7	0.23	0.00	0.38%	0.04%
STA23 24-28cm	18-jul	155.3	5.8	93	7	0.21	0.00	0.35%	0.04%
STA23 28-32cm	18-jul	143.4	4.5	88	4	0.22	0.00	0.25%	0.05%
STA23 32-36cm	18-jul	115.4	4.3	62	8	0.24	0.00	0.36%	0.05%
STA23 36-40cm	23-aug	87.1	1.1	59	6	0.22	0.00	0.26%	0.05%

Table 16 : Results for sediment samples including uncertainties from AMS counting statistics

* No tracer was added to this sample, and therefore no results for the activity concentrations could be found.

Appendix III: The Rongelap and the Bikini Atoll

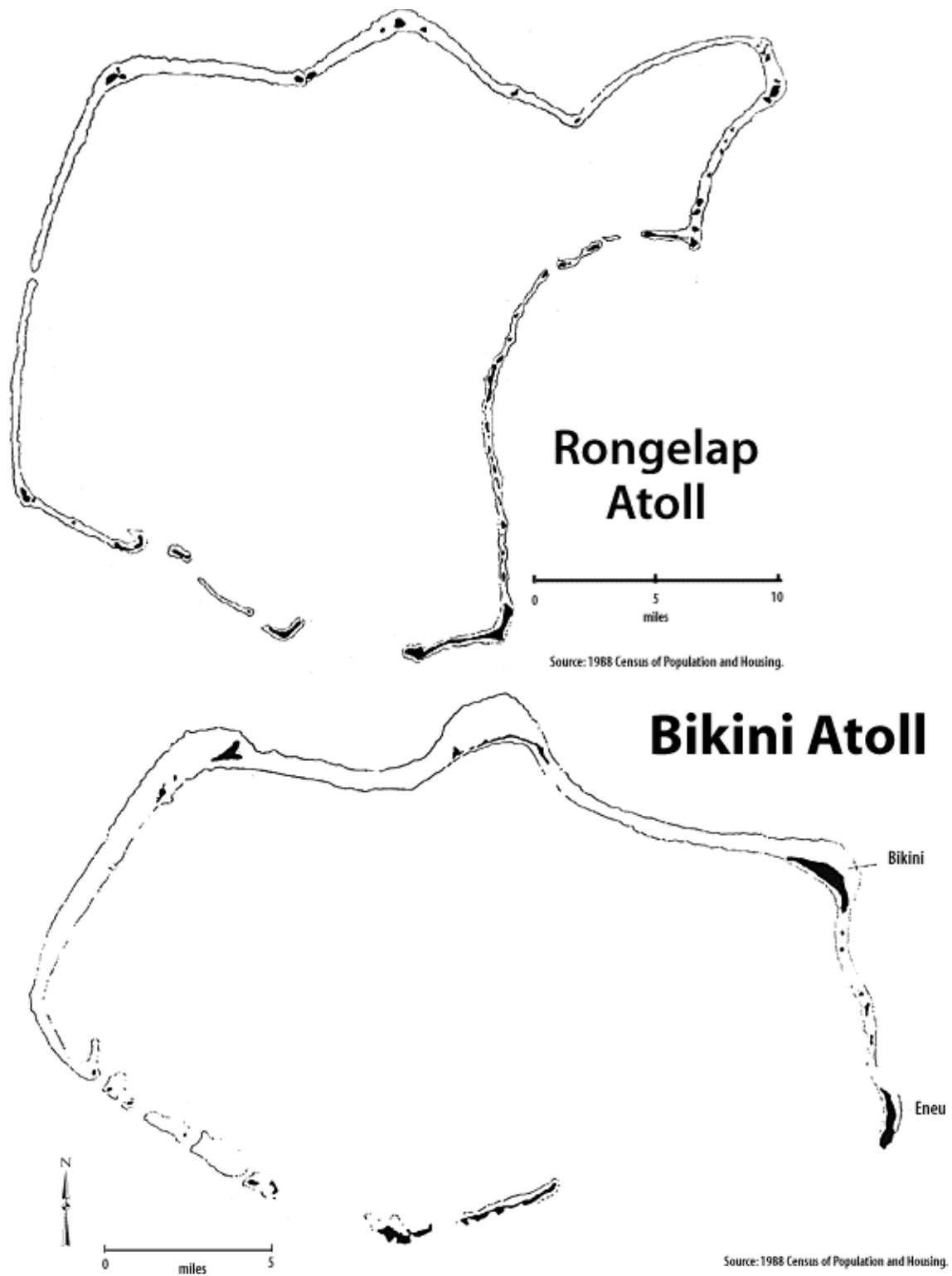


Figure 24: The Bikini and the Rongelap Atoll